



저작자표시-비영리-변경금지 2.0 대한민국

이용자는 아래의 조건을 따르는 경우에 한하여 자유롭게

- 이 저작물을 복제, 배포, 전송, 전시, 공연 및 방송할 수 있습니다.

다음과 같은 조건을 따라야 합니다:



저작자표시. 귀하는 원저작자를 표시하여야 합니다.



비영리. 귀하는 이 저작물을 영리 목적으로 이용할 수 없습니다.



변경금지. 귀하는 이 저작물을 개작, 변형 또는 가공할 수 없습니다.

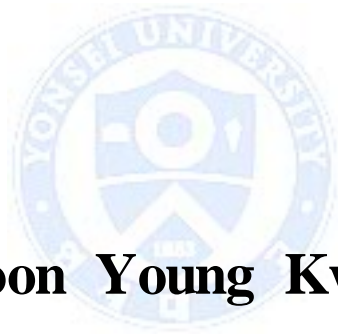
- 귀하는, 이 저작물의 재이용이나 배포의 경우, 이 저작물에 적용된 이용허락조건을 명확하게 나타내어야 합니다.
- 저작권자로부터 별도의 허가를 받으면 이러한 조건들은 적용되지 않습니다.

저작권법에 따른 이용자의 권리는 위의 내용에 의하여 영향을 받지 않습니다.

이것은 [이용허락규약\(Legal Code\)](#)을 이해하기 쉽게 요약한 것입니다.

[Disclaimer](#)

**A study on the new revision total knee
prosthesis development with an
assessment on the biomechanical stability
and the biological safety**



Soon Young Kwon

**Department of Biomedical Engineering
The Graduate School, Yonsei University**

**A study on the new revision total knee
prosthesis development with an
assessment on the biomechanical stability
and the biological safety**

**A Dissertation Thesis Submitted to the Department of
the Department of Biomedical Engineering, the Graduate
School of Yonsei University in partial fulfillment of the
requirements for the degree of Doctor of Philosophy**

Soon Young Kwon

June 2015

**This certifies that the Dissertation
Thesis of Soon Young Kwon is approved.**

Thesis Supervisor : Jong-Chul Park

Thesis Committee Member #1 : Nam-Hyun Kim

Thesis Committee Member #2 : Sun Kook Yoo

Thesis Committee Member #3 : Jungsung Kim

Thesis Committee Member #4 : Dohyung Lim

The Graduate School

Yonsei University

June 2015

TABLE OF CONTENTS

ABSTRACT	vi
I. INTRODUCTION	
1. Anatomy of the Knee	01
2. Biomechanics of the Knee	06
3. Primary Total Knee Arthroplasty	11
4. Revision Total Knee Arthroplasty	18
5. Outline of This Research	20
II. DESIGN ELEMENT ANALYSIS AND DESIGN OF A REVISION TOTAL KNEE REPLACEMENT PROSTHESIS	
1. Design Element Analysis and Design according to the Clinical Requirements ..	22
2. Structural Stability Evaluation of the Revision Knee Replacement Prosthesis by Component Part	29
III. BIOMECHANICAL STABILITY EVALUATION ON THE REVISION KNEE REPLACEMENT PROSTHESIS	
1. Evaluation of the Mechanical Stability of the Proposed Revision Total Knee Replacement Prosthesis	35
2. Finite Element Modeling and Biomechanical Analysis of Surgical Outcomes	44
IV. BIOLOGICAL SAFETY EVALUATION	
1. Cytotoxicity Test	56
2. Intracutaneous(intradermal) Reactivity Test	59
3. Irritation and Skin Sensitization Test	63
4. Acute Systemic Toxicity Test	67
5. Genotoxicity Test (bacterial reverse mutation test-Ames test)	70
V. CONCLUSIONS AND FUTURE WORK	75
REFERENCE	81
ABSTRACT (IN KOREAN)	85

LIST OF FIGURES

Figure 1.	The shape of the distal femur(Right)	2
Figure 2.	The locations of ligament attachments in knee joint	2
Figure 3.	The shape of patellar	3
Figure 4.	The muscles in the knee joint(anterial view)	4
Figure 5.	The ligaments in the knee joint	6
Figure 6.	The motions of the knee joint	7
Figure 7.	The rolling and gliding in flexion & extension in the knee joint	7
Figure 8.	The range of motions in flexion and extension in the knee joint	9
Figure 9.	The reaction force in the patellofemoral joint	10
Figure 10.	The several diseases for the total knee arthroplasty	12
Figure 11.	Operation cases of total knee arthroplasty in domestic(Statistical data in HIRA, Korea)	12
Figure 12.	The components of an artificial knee replacement	13
Figure 13.	The result of consulting with SF-26, PASE	15
Figure 14.	The survival rate since artificial knee operation(Weir et al)	16
Figure 15.	The survival rate since artificial knee operation(Gill et al)	16
Figure 16.	Overall incidences in total knee arthroplasty in 2002 and 2012	17
Figure 17.	The failure reasons in the total knee arthroplasty	18
Figure 18.	The global market forecast to 2019 in total knee replacement	20
Figure 19.	The Korea market forecast in total knee replacement	20
Figure 20.	The design concepts in a new revision total hip replacement.	21
Figure 21.	The design parameters in range of motion of new R-TKR	23

Figure 22.	The design parameters in conformity with femoral component and tibial insert of new R-TKR	23
Figure 23.	The design parameters in stem extension	24
Figure 24.	The design parameters in stem extension and offset adaptor	25
Figure 25.	The design parameters in femur & tibia blocks for bone deficit	26
Figure 26.	The design parameters in jump distance and rollback between femur & inserts components	27
Figure 27.	The design parameters in insert locking rod and spiral lock system	28
Figure 28.	The test methods including loading condition for structural combination stability in femur and tibia component with extension stem	33
Figure 29.	The fatigue testing with tibial baseplate according ASTM F 1800-12	37
Figure 30.	A slight plastic deformation of specimen 1.1 after 3605 load cycles ³ at load level 9	39
Figure 31.	Load and displacement(min/max) curves by number of loading- specimen 1	39
Figure 32.	Representative graphs for load and displacement(min/max) by number of loading cycles - specimen 2	40
Figure 33.	The assembly/disassembly locking test with offset adaptor and stem extension	41
Figure 34.	The measurement of assembly and disassembly torques with SCHATZ machine	42
Figure 35.	Patient's tibia geometry and insertion R-TKR within tibia	45
Figure 36.	Surgical FE models according right location within tibia geometry	46
Figure 37.	The loading condition and constrain conditions in FEM (a)Loading Condition (2000N), (b)Fixed Condition (20mm)	47

Figure 38.	The measurements of the stress and strain in tibia cortical and cancellous bone	48
Figure 39.	Comparison of strain distribution within implanted proximal tibia	49
Figure 40.	The strain distribution in the tibia cortical bone(Model A : new R-TKR, Model B - commercial R-TKR)	53
Figure 41.	The strain distribution in the tibia cancellous bone(Model A : new R-TKR, Model B - commercial R-TKR)	54
Figure 42.	The image of the stem plug	55
Figure 43.	The results of the cytotoxicity test	58
Figure 44.	Relative cell viability of the cytotoxicity test	59
Figure 45.	The injection thermal site in intracutaneous(intradermal) reactivity test	60
Figure 46.	The procedure of the irritation and skin sensitization test	65
Figure 47.	The results of the irritation and skin sensitization test	66
Figure 48.	Acute systemic toxicity test result : no mices with death, abnormality and body weight loss	69
Figure 49.	The body weight changes on acute systemic toxicity test	70

LIST OF TABLES

Table 1.	The classification of bone loss after the removal of total knee arthroplasty(Anderson Orthopedic Research Institute : AORI)	19
Table 2.	The test methods including loading condition for structural stability	30
Table 3.	The results in stress distribution in component of new R-TKR	31
Table 4.	The results in stress distribution in femur and tibia united extended stem FE model	34
Table 5.	The fatigue test methods according to ASTM 1800-12	36
Table 6.	Progressive fatigue loading for specimen 1.1	37
Table 7.	Results for specimen 1 (Tested by progressive loading)	38
Table 8.	The result of assembly locking tests	43
Table 9.	Mechanical properties for finite element model	45
Table 10.	Evaluation criteria of the cytotoxicity test	57
Table 11.	The results of the cell viability and reactivity grade in the cytotoxicity Test	58
Table 12.	Dermal observation scoring in intracutaneous reactivity test	61
Table 13.	The results of intracutaneous reactivity test	62
Table 14.	The preparation of irritation and skin sensitization Test	64
Table 15.	Magnusson and Kligman scale	65
Table 16.	Negative control, test article extract, and positive control observation after challenge phase	66

Table 17.	Acute systemic toxicity test materials	67
Table 18.	Acute systemic toxicity test condition	68
Table 19.	Acute systemic toxicity test result	69
Table 20.	Bacterial Reverse Mutation Test - Ames test materials	71
Table 21.	S-9 mixture condition	72
Table 22.	Ames plate incorporation assay For 0.9% sodium chloride(saline) extract	73
Table 23.	Ames plate incorporation assay For 4% dimethyl sulfoxide (DMSO) extract	74



ABSTRACT

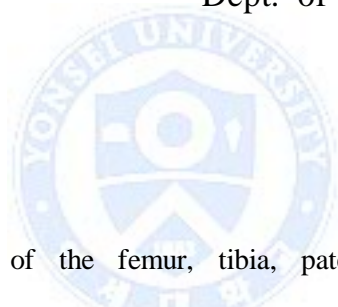
A study on the new revision total knee prosthesis development with an assessment on the biomechanical stability and the biological safety

Soon Young Kwon

Dept. of Biomedical Engineering

The Graduate School

Yonsei University



The knee joint consists of the femur, tibia, patella, articular cartilage, and ligaments and is one of the largest joints in the human body. The knee joint is constantly subjected to repeated weight-bearing loads and is prone to injury or functional decline. In severe cases, such as degenerative arthritis, degenerative knee joint arthritis, rheumatoid arthritis, and trauma where conservative therapies show little improvement, total knee arthroplasty (TKA) has proven to be an efficient treatment option with good clinical outcomes. Revision TKR is required when the life span of the device implanted during the primary TKR has expired, and this method can serve as a suitable knee joint replacement procedure when different functional requirements (mechanical, clinical, and design) are needed or harsh conditions need to be overcome.

In an effort to improve the service life of knee replacements, extensive studies have been conducted and a wide range of products have been commercialized. In Korea, the several primary TKR was already developed and commercialized, but the supply of revision TKR prostheses depends on imports from global companies, and revision TKR prostheses require domestic research and development.

This study was conducted to analyze the clinical and mechanical design elements of revision total knee replacement systems based on the primary artificial knee joints currently in use and to develop a new revision TKR prosthesis by performing various tests and evaluations. To implement the design of a new revision TKR prosthesis, three design elements, namely stability, modularity, and safety, were taken into account in analyzing the detailed design elements and product design. In order to increase stability, the range of motion of the prosthesis was restricted with high conformity. Furthermore, the femur stem extension, tibial baseplate, and stem extension were anatomically designed to enhance the support provided by our revision TKR system. To restore bone removal and loss, reconstruction parts were introduced in order to compensate and the tibial insert post was concavely designed, which increases the jump distance and prevents dislocation.

We performed a number of tests to evaluate this new revision TKR system wherein several prosthesis design parameters were considered. Structural stability was validated using finite element analysis (ABAQUS v6.10) and performed ASTM F1223-08 and F1800-07 and compared with the primary TKR system. The stress distribution results showed that the strength of the femoral component was 30% higher with the new revision TKR system than with the primary TKR system. Eccentric test results showed that the strength of the tibial baseplate was 23% lower compared with the primary TKR system, but this factor does not significantly affect

stability considering the yield stress of CoCr and high load level.

We conducted a tibial cyclic fatigue test and a stem extension assembly locking test to assess the tibial components. Fatigue load was applied to the proposed TKR prosthesis in accordance with the ASTM test method to investigate the failure feature. No fracture or crack was observed, even under the application of a load higher than the ASTM guideline standard. The bond strength between the stem extension and offset adapter was tested by the assembly and disassembly torque test. The result indicated an assembly-to-disassembly torque ratio ranging between 99.7% and 101% (average: 100.5%), thus demonstrating that stability was sufficiently reflected in the proposed revision TKR prosthesis.

After TKR implantation, the major parameters for stability analysis include the load transfer of the knee and biomechanical characteristics. It is well known that the stress concentration and stress shielding induced by knee replacement during insertion can cause fracture, pain, and loosening induced by bone resorption. Thus, load distribution in the tibia is an important factor from the biomechanical point of view. We used computed tomography to reconstruct surgical finite element models in order to assess the influence of loading distribution with stress/strain. First, the stress analysis results showed that the new revision TKR system had lower than yield strength at the tibia baseplate, stem extension, and cortical and cancellous bone it means that the proposed TKR prosthesis does not need any additional improvement or supplement in design elements for application. As such, structural stability is sufficiently provided under the aspect of tibial fracture risk. Second, the stress-strain distribution at the cortical bone was high at the proximal posterior and distal anterior portions, whereas that at the cancellous bone was high at the proximal posterior and distal lateral portions. The pattern of the a real-life revision

TKR system was similar to that of the new revision TKR system. This implies that adequate stress/strain can be generated in the cortical and cancellous bones during the insertion of the proposed revision TKR, which is expected to mitigate the loosening-related problem due to stress-shielding effects and increase in bone resorption and remodeling, which would not cause bone loss or instability.

Since an artificial knee joint is a medical device that is inserted into the human body for a long period of time, its biological safety should be ensured. For the development of a new revision TKR prosthesis, the hole plug, for which metal is usually used, was fabricated with a new material, SL7870 and its biological safety was validated in the cytotoxicity, subcutaneous (intradermal) reactivity, sensitization, acute systemic toxicity, and genotoxicity tests. The cytotoxicity test revealed that the extract of the test material was non-toxic by verifying 99% cell viability. In the subcutaneous (intradermal) reactivity test using rabbits, the extract of the test material did not trigger skin reactions such as erythema, crusting, and swelling. Nor did the sensitization test reveal any abnormal reactions on the skin of the mice exposed to stimuli. The acute systemic toxicity test did not trigger any abnormal changes in skin, hide, eyes, and body weight. Finally, in the genotoxicity test, no significant differences were observed in the results of mutagenicity of microorganisms between the test material and negative controls. The biological safety of the new material was thus proved.

The clinical and anatomical requirements for revision TKR prostheses were analyzed for the purpose of developing a new revision TKR prosthesis. Detailed parameters for important factors were analyzed, and a design meeting all the requirements was implemented. A variety of validation and testing methods were established in order to evaluate whether the designed product meets the functional

and biomechanical requirements. We evaluated our new revision TKR system using structural, mechanical, and biological tests in order to assess whether it meets functional and key requirements. In analysis results of various performed tests, we confirmed the feasibility of our new revision TKR system and verified its clinical applicability and marketability. Furthermore, This study is significant in that it first provided the basic data for the development of a domestically produced revision TKR prosthesis. Based on the results of this study, research will be continued with the intent to obtain approval for the proposed revision TKR prosthesis through its efficacy validation and clinical trials. The achievement of this study is expected to contribute to the research and development of domestically produced revision TKR prostheses for the domestic and global market sharing, which is currently dominated by imported products. It is hoped that our results will be used as a foundation for the local TKR market, which predominantly includes foreign products.

Key words : total knee arthroplasty, artificial knee joint, Revision total knee replacement prosthesis, development, designs, biomechanical stability, biological safety, evaluation, finite element method, mechanical test, stress

CHAPTER I. INTRODUCTION

1. Anatomy of the Knee

In the human body, the knee joint transmits body weight from the upper body to the feet, provides range of motion (ROM) to the lower leg, and maintains momentum. Situated between the two longest lever-like bones in the body and constantly exposed to the heavy load of body weight, the knee joint is at high risk of strain and injury. This chapter addresses the anatomic details of the knee joint necessary for designing a revision total knee replacement (TKR) prosthesis. Specifically, the bone structure, muscles, menisci, and ligaments of the knee joint are described in sections 1.1, 1.2, 1.3, and 1.4, respectively.

1.1 Bone Structure

The knee joint is formed by three bones: the femur, tibia, and patella. The part of the femur forming the knee joint is the distal femur. The distal femoral condyle has an asymmetric shape and size and its posterior aspect is separated into medial and lateral condyles by the intercondylar notch.¹⁾²⁾(Fig.1)

The proximal tibia, which, with the femur, forms the tibiofemoral joint of the knee, is composed of medial and lateral condyles, which are separated by the intercondylar eminence. The medial condyle is almost flat, while the lateral condyle is concave. In the center of the intercondylar eminence, there are structures that connect the different components of the knee joint: the anterior horn of the medial meniscus, the anterior cruciate ligament, the posterior horn of the lateral meniscus, the posterior horn of the medial meniscus, and the posterior

cruciate ligament, to name them in anteroposterior order²⁾(Fig.2).

The patella is the largest sesamoid bone and has the thickest layer of cartilage in the human body (Fig. 3). It forms the patellofemoral joint with the femur and protects the knee joint from the frontal side. The patella increases the functional lever arm of the quadriceps muscle group and thus facilitates knee joint extension. It also distributes the pressure exerted on the femoral condyle and reduces friction between the patella and the femur.¹⁾

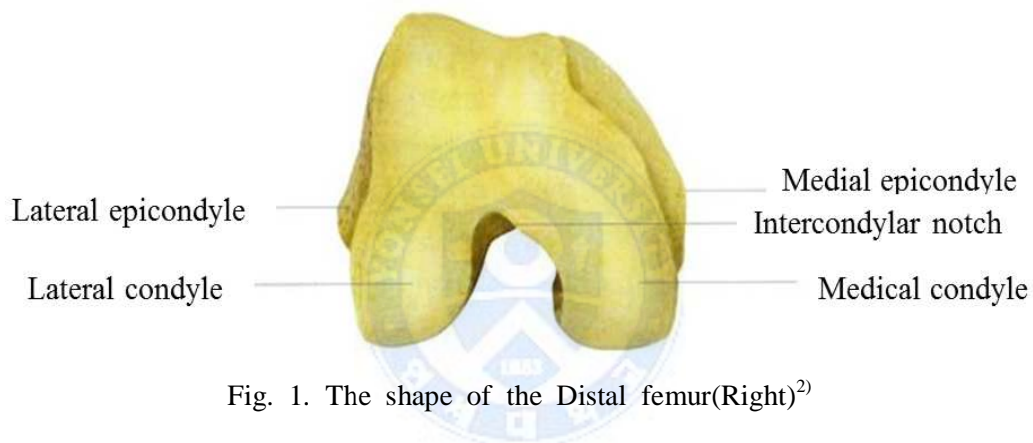


Fig. 1. The shape of the Distal femur(Right)²⁾

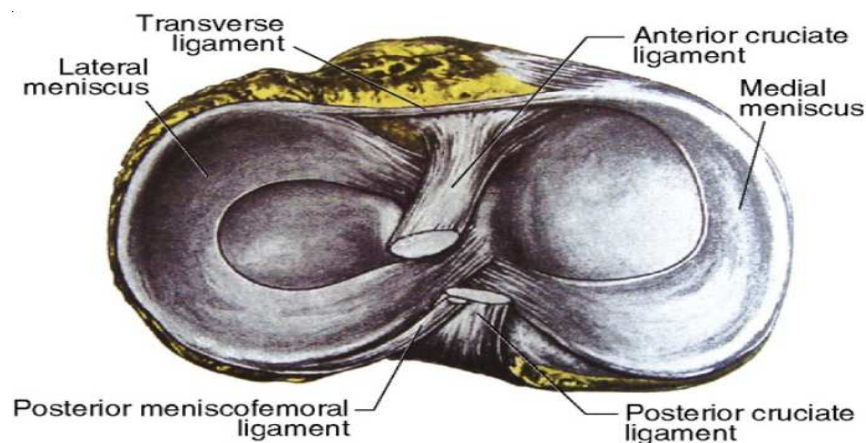


Fig. 2. The locations of ligament attachments in knee joint³⁾

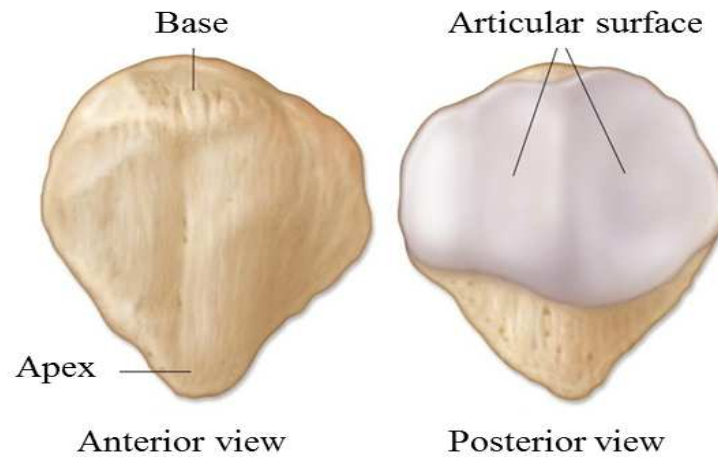


Fig. 3. The shape of patellar⁴⁾

1.2 Muscles

The femoris consists of four muscles (rectus femoris, vastus lateralis, vastus medialis, and vastus intermedius) that are extensors of the knee joint. The rectus femoris has two tendinous origins on the distal ilium and insertion points on the patella. The vastus lateralis, the largest muscle of the quadriceps group, begins as a broad aponeurosis in the proximal part of the intertrochanteric line and extends down to the center of the linea aspera on the femur. Its distal part is attached to the lateral border of the patella. The vastus medialis is divided into the vastus medialis obliquus and the vastus medialis longus and originates from the lower half of the intertrochanteric line and attaches to the medial border of the patella. The vastus intermedius originates at the anterior and lateral femoral shaft. The quadriceps muscles are attached to the tibia by the patellar ligament extending over the patella.¹⁾²⁾(Fig. 4)

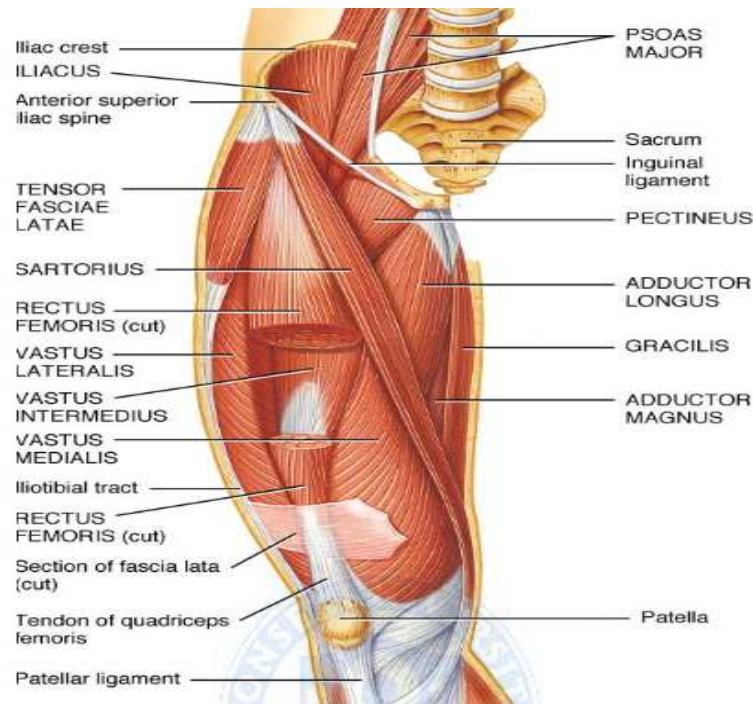


Fig. 4. The muscles in the knee joint(anterial view)⁵⁾

1.3 Meniscus

The medial and lateral menisci are two C-shaped disks of fibrocartilage that cover about 2/3 of the tibia's surface. A meniscus is composed of densely packed collagen (75%), non-collagenous protein (8–13%), and fibrocartilage consisting of fibroblasts and chondrocytes. The dense annular array of collagen fibers is optimally formed to absorb efficiently the hoop stress of weight-bearing exerted on the knee joint. Furthermore, the radial array in the proximal and middle parts can efficiently provide structural support for rigidity and resistance against longitudinal splitting. The lateral meniscus has higher shear strength and more rigidity than does the medial meniscus.¹⁾

1.4 Ligaments

The connective stability of the knee joint components is provided by four ligaments: the anterior and posterior cruciate ligaments (ACL/PCL) as well as the lateral and medial collateral ligaments (LCL/MCL). Each ligament performs the function of preventing knee joint dislocation.²⁾⁸⁾

The ACL originates from the tibial intercondylar eminence and inserts posterolaterally onto the lateral condyle of the femur. As knee flexion occurs, the ACL becomes increasingly more twisted, providing the knee with primary protection from anterior dislocation of the tibia within its entire ROM. It also limits hyperextension and tibial rotation.

The PCL is located at the lateroposterior surface of the medial condyle of the femur and runs toward the tibia almost vertically. Its shear strength is 1.5- to 2-fold higher than that of the ACL. As knee extension occurs, its anterior portion, which occupies most of its surface, becomes loose, with the posterior portion partially tightening. Conversely, it tightens in flexion, with the posterior portion partially loosening. Given that the PCL provides about 95% of the total restraint to posterior translation from the femur to the tibia, the PCL plays an important role from the biomechanical viewpoint.²⁾

The LCL runs from the posterior part of the lateral epicondyle of femur to the lateral fibular head. The MCL has superficial and deep components. The superficial MCL fibers attach proximally to the medial femoral epicondyle and distally to the medial aspect of the tibia. They are also connected to the articular capsule and medial meniscus. The MCL is tense in extension and loose in flexion. Both the LCL and MCL function to prevent lateral translation of the knee joint²⁾⁸⁾(Fig.5).

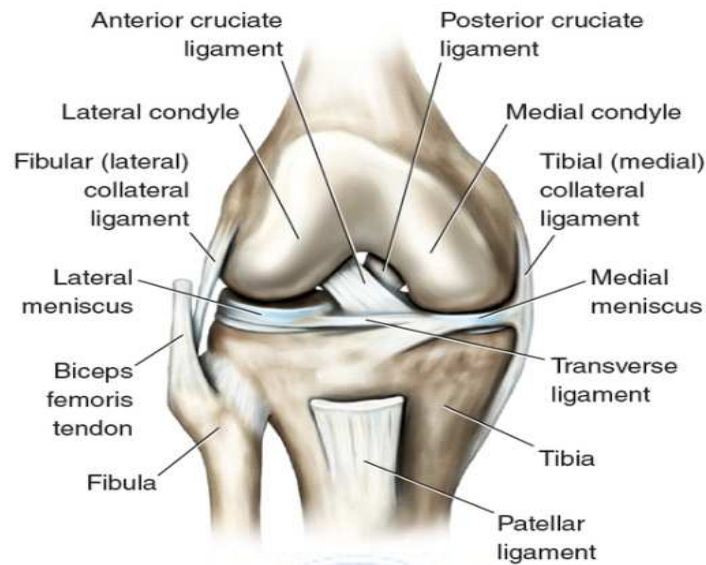


Fig. 5. The ligaments in the knee joint⁶⁾

2. Biomechanics of the Knee

The knee joint moves in the sagittal, coronal, and transverse planes. The biomechanics of the knee may involve quantifying the force generated by one muscle group when executing a motion in one plane, investigating a knee exercise, or evaluating the magnitude of force and moment in the knee joint. In this section, the biomechanical features of the joints of the knee joint complex that are important as design elements of an artificial knee joint are described.

2.1 Tibiofemoral joint

From the kinematic point of view, the tibiofemoral joint is a sort of pivotal hinge joint whose analytical structures, such as its ligaments and surrounding muscles and articular capsule, allow six degrees of freedom: three translations (medial-lateral,

anterior-posterior, and proximal-distal) and three rotations (flexion-extension, internal-external, and varus-valgus) (Fig. 6). Stability during each knee motion in full extension is provided by the anterior part of the collateral and cruciate ligaments and menisci as well as the knee-locking of the femoral and tibial condyles.²⁾⁹⁾

The initiation of knee flexion unlocks the knee, and the contraction of the popliteus muscle allows lateral rotation of the femur on the tibia. The initial flexion occurs primarily as rolling of the femoral condyles on the tibia. As flexion continues, however, gliding takes place as the primary motion⁹⁾ (Fig. 7).

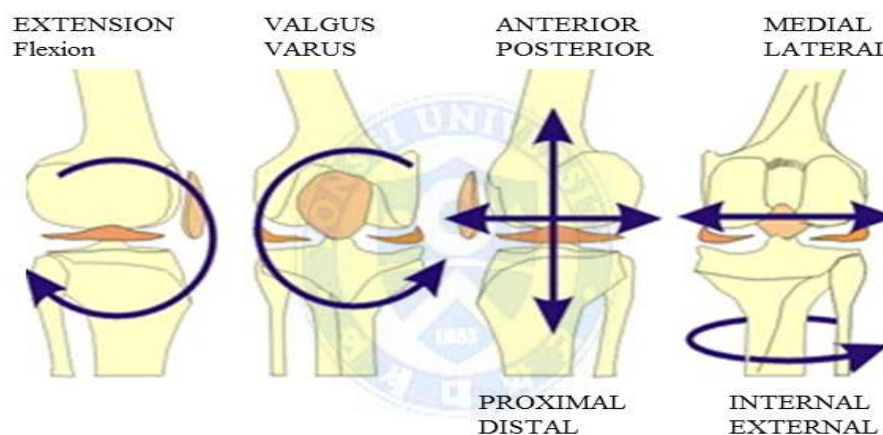


Fig. 6. The motions of the knee joint²⁾

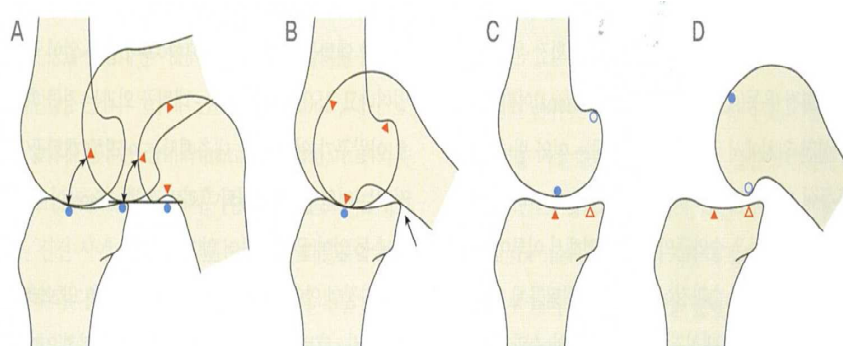


Fig. 7. The rolling and gliding in flexion & extension in the knee joint²⁾

The menisci are fixed on the articular surface during extension, but move posteriorly during flexion, with such anterior-posterior translation occurring more markedly in the lateral meniscus than in the medial meniscus up to 12 va. 6mm. The articular surface of the medial femoral condyle has a longer anteroposterior length than that of the lateral femoral condyle, so that the lateral compartment reaches full extension faster than does the medial compartment. This triggers $\sim 15^\circ$ oblique spiral rotation accompanying the medial rotation of the lateral femoral condyle on the tibia to complete the final 20° extension. Along with soft tissue, this structure provides primary restraint to knee joint motion and prevents the knee from exceeding the normal ROM.²⁾ The knee joint ROM in the sagittal plane is between 0° (full extension) and 140° (full flexion) (Fig.8).

From a kinetic point of view, the tibiofemoral joint is exposed to both compressive and shear forces. The pressure exerted on the tibiofemoral joint is known to be 3- and 4-fold greater than body weight in a standing position and while climbing stairs, respectively. The medial aspect of the superior articular surface of the tibia supports most loads under knee extension. However, given that the contact surface of the medial aspect of the superior articular surface of the tibia is larger than its lateral aspect by about 60%, the stress exerted on the joint remains manageable even when the load is distributed to the medial aspect. Furthermore, the medial articular cartilage is three times as thick as the lateral aspect, thus protecting the joint from abrasion.

Shear force occurs when knee flexion increases to 90° . Once shear force is generated, it tends to displace the femur posteriorly on the superior articular surface of the tibia and encounters resistance from ligaments and other supporting structures.⁹⁾

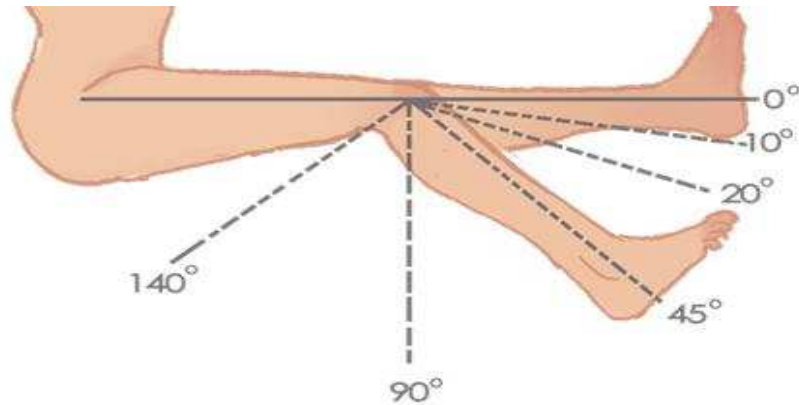


Fig. 8. The range of motions in flexion and extension in the knee joint⁷⁾

2.2 Patellofemoral joint

Kinetic analysis of patellofemoral joint extension from full flexion reveals that the patella glides about 7 cm downwards on the femoral condyle. When the knee flexes to 140° from full extension, both the medial and lateral aspects of the femur form the patellofemoral joint with the patella. If flexion exceeds 90°, the patella rotates laterally and only the medial aspect of the femur is involved in forming the patellofemoral joint with the patella. In full flexion, the patella glides deeper into the intercondylar groove.⁹⁾

From the kinematic viewpoint, the most important function of the patella is its pulley mechanism, which enhances the efficiency of the quadriceps muscle group by increasing the lever arm during extension. Due to the fact that the patellar tendon is located anteriorly to the tibiofemoral joint by the thickness of the patella, the knee can be extended more efficiently owing to the extended lever arm of the quadriceps muscle group²⁾(Fig. 9). The load exerted on the patellofemoral joint increases as flexion continues, i.e., as the flexion moment arm

increases, because the tension between the quadriceps tendon and the patellar tendon decreases as the angle formed by their axes becomes smaller. The load on the patellofemoral joint increases in proportion to the degree of flexion to 1.5-fold and 6-fold higher than body weight at 30° and 90° flexion, respectively, with respect to the straight-leg state.¹⁰⁾ The magnitude of the load there by exerted on the patellofemoral joint changes according to its functional activities; for example, 0.5, 3.3, and 7–8 times body weight during walking ,stairclimbing, and squatting, respectively.

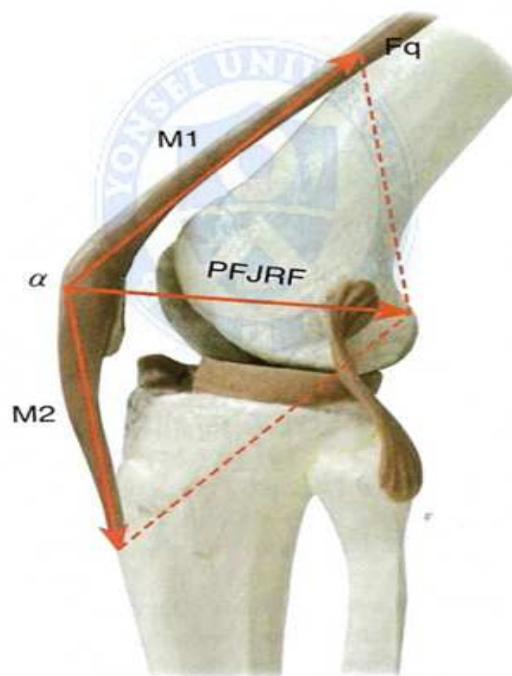


Fig. 9. The reaction force in the patellofemoral joint²⁾

3. Primary Total Knee Arthroplasty

The basic concept of primary total knee arthroplasty (TKA) is to recover normal function of the knee joint by restoring the damaged articular surface. TKR was developed to respond to the basic human desire to bend and extend the knee without pain while executing daily activities by replacing the joint with an artificial joint when individuals are impeded by injury- or disease-induced limited ROM. This section addresses the details associated with TKA, such the history of artificial knee joint development, surgical outcomes, and survival rates.

3.1 Current status of primary total knee arthroplasty

The typical diseases for which TKA is applicable are osteoarthritis, rheumatoid arthritis, osteonecrosis, ankylosis, and Charcot joint.¹¹⁾ These diseases cause pain and a substantially reduced ROM of the knee joint. While various conservative treatments are primarily administered, TKA is opted for as the last resort if conservative therapies fail. Additionally, the number of TKA cases is increasing globally as a result of the increasing prevalence of degenerative arthritis,¹²⁾ also known as senile arthritis, due to the steadily growing elderly population.¹³⁾(Fig. 10)

In Korea, TKA has been rapidly increasing since 2006. According to the 2013 major surgical statistics data collected by the National Health Insurance TKAs in 2013 was 54,000, an increase of 43% compared to 2006. This trend was also observed across the world; for example, there were 70,000 TKAs in 2009 in the UK¹⁴⁾ and 40,000 in 2003 in the USA, with an increase of 673%(3,000,000cases) predicted for 2030.¹⁵⁾(Fig. 11)

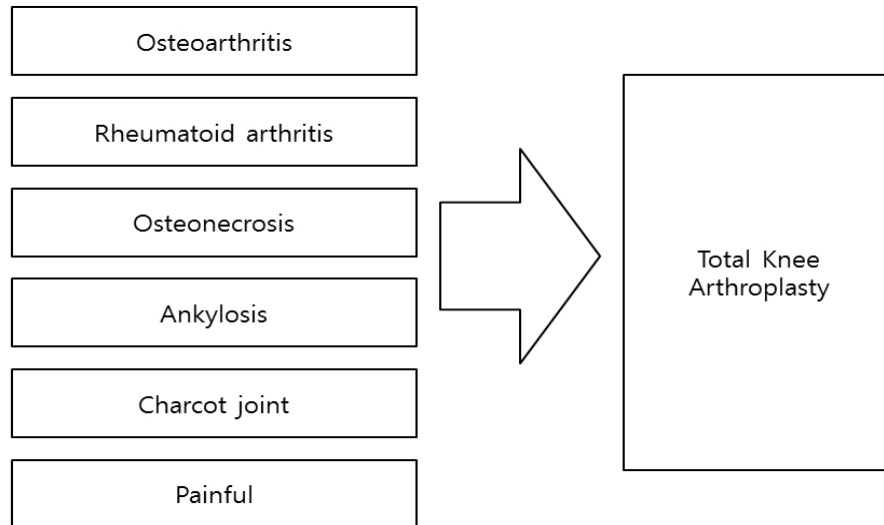


Fig. 10. The several diseases for the total knee arthroplasty

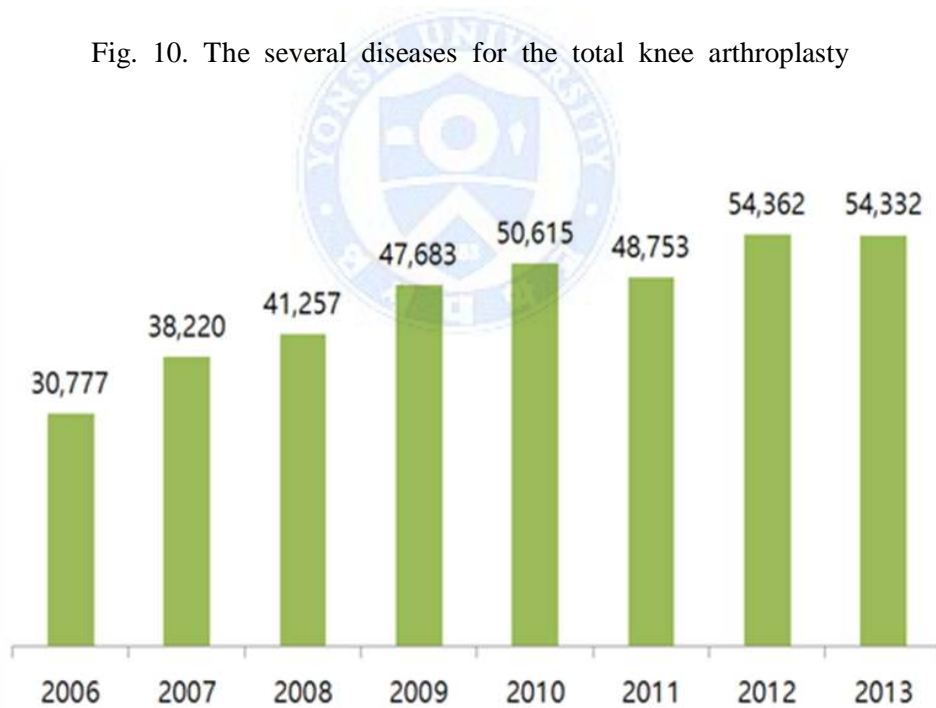


Fig. 11. Operation cases of total knee arthroplasty in domestic(Statistical data in HIRA, Korea)

3.2 Development and progress of the artificial knee joint

In the initial development phase of artificial knee joints, the articular surface was resurfaced with soft tissues, not metal or polyethylene (PE). The first attempt at interposing soft tissue to construct the articular surface was made in 1860 by Verneuil, followed by a series of unsuccessful attempts at similar interposition arthroplasty using a swine urinary bladder, femoral fascia, a patellar tendon mucous membrane, nylon, and cellophane. In 1940, driven by the fairly successful hip arthroplasty using metal cup liners, metal-based knee arthroplasty was introduced. The current concept of knee replacement began with the unicondylar, bicondylar, or hinged type (Fig. 12).²⁾

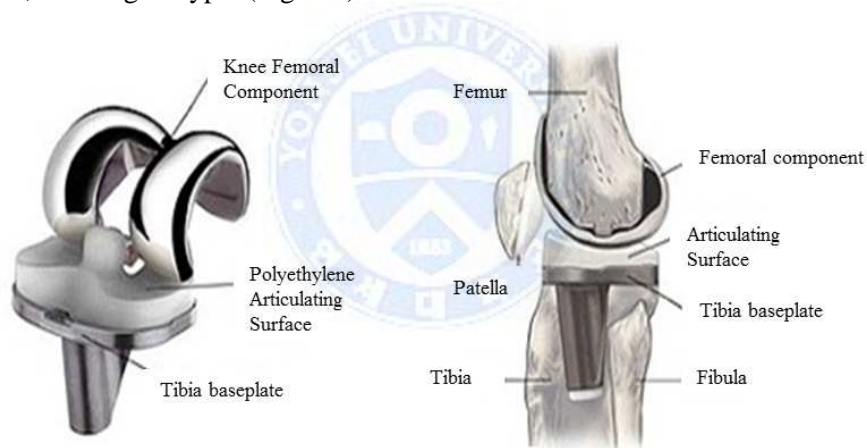


Fig. 12. The components of an artificial knee replacement

The 1970s saw the development of metal-on-PE knee replacement. Freeman et. al¹⁶⁾ specified the following criteria for knee prosthesis production: 1) the salvage procedure should be simple to execute; 2) the mass of the inserted prosthesis should be equal to that of the bone removed in primary arthrodesis of the joint, and the large and flat surfaces of the cancellous bone should be left intact; 3)

torsion, adduction, or abduction moment should not be transmitted through the prosthesis–bone interface; 4) friction should be minimal; 5) loading should be distributed over the maximum possible surface area when fixing the prosthesis to the bone; and 6) abrasion byproducts should be minimal.²⁾¹⁶⁾

In the late 1970s and early 1980s, extensive studies were carried out on knee replacement implant materials and methods, such as tibial metal backing to improve fixation, modularization to simplify application, and cementless fixation to improve durability. The late 1980s saw the development of cemented and cementless stem fixation and metal wedges, taking into account bone loss and soft tissue instability in revision TKA. Research on replacement implants has continued up to present times, focusing on abrasion minimization and knee joint ROM maximization by optimizing the design of replacement implants.²⁾¹⁷⁾

3.3 Surgical outcomes of total knee arthroplasty

The superior surgical outcomes of TKAs and the survival rate of the artificial knee joints have been verified in many clinical studies.¹⁸⁾¹⁹⁾²⁰⁾ In a postoperative follow-up study conducted by Th. Tsonga,²¹⁾ Greek elderly women who underwent primary TKA were surveyed. The improvement in postoperative quality of life and physical activity was assessed using the Medical Outcomes Study Short Form(SF-36) and the Physical Activity Scale for the Elderly(PASE). The average SF-36 questionnaire score increased by about 52%, from 29.33(preoperative level) to 62.35 (6-month postoperative level). The score for the PASE questionnaire increased by 36%, from 43.3 to 67.9(Fig. 13). The results of the 6-month follow-up of TKA patients revealed that improvement was found especially in pain, physical function, and vitality scale.²¹⁾

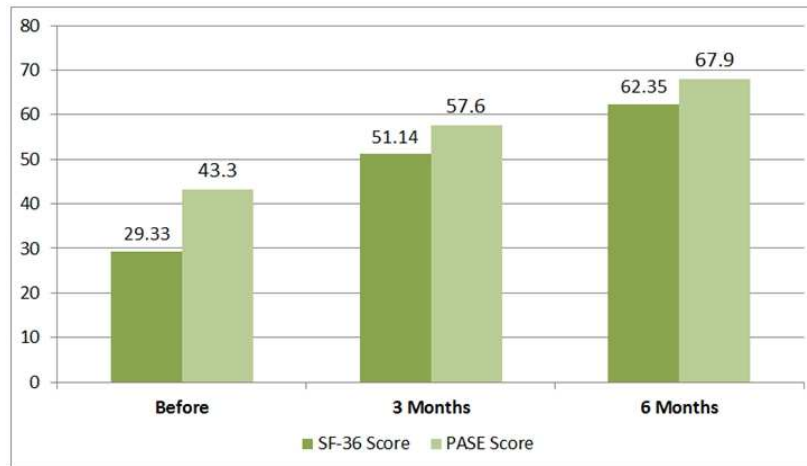


Fig. 13. The result of consulting with SF-26, PASE²¹⁾

Weir²²⁾ and Gill²³⁾ reported on the survival rates of the primary artificial knee joint. Weir conducted a follow-up study of 208 TKA cases for 15 years, and Gill followed 404 cases for 17 years. In both follow-up studies, the 10-year survival of the knee prosthesis exceeded 90% (Figs. 14 and 15). The results of the clinical assessments of pain, ROM, stability, and functionality also demonstrated an 89.6% improvement, from 36 points preoperatively to 90 points postoperatively.²²⁾

Gill stated that the design of the artificial knee joint was progressing toward positive long-term effects and noted that soft tissue conservation and the controversial aspects between biomechanical and clinical outcomes were issues yet to be resolved.²³⁾

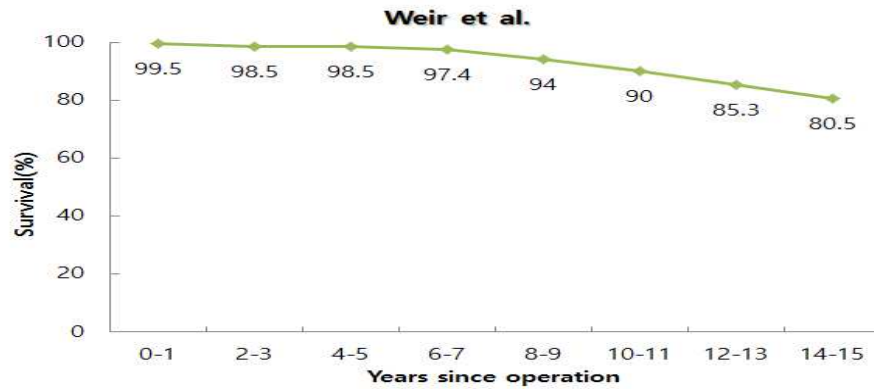


Fig. 14. The survival rate since artificial knee operation(Weir et al)²²⁾

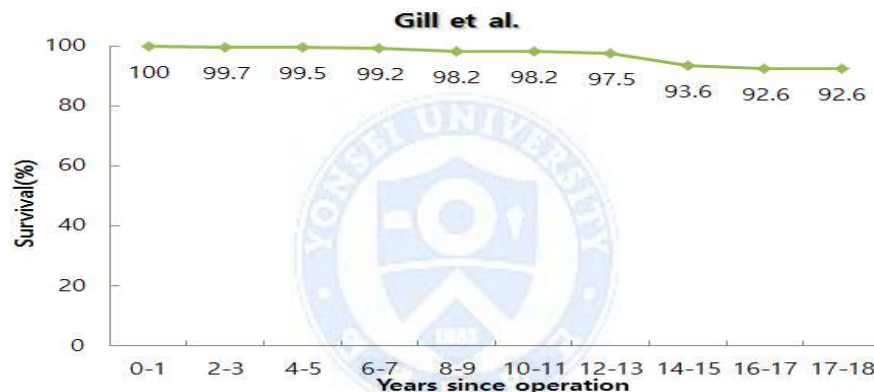


Fig. 15. The survival rate since artificial knee operation(Gill et al)²³⁾

3.4 Mechanisms of knee replacement failure

Sharkey analyzed the frequency and causes of failure of primary TKA in two consecutive studies. Their 2002 report on the follow-up of 212 revision TKAs over a period of three years (1997–2000) and their 2014 report of a 10-year follow-up (2003–2012) of 781 revision TKAs focused on the failure rates of primary TKA according to their failure mechanisms²⁶⁾²⁷⁾(Fig. 16).

Aseptic loosening was identified as the most common cause of failure in both

reports. Likewise, in Australian and Swedish annual reports of knee arthroplasty for 2011, aseptic loosening was shown to account for over 20% of all causes of failure. Sharkey ascribed the etiology of this failure mechanism to the methods used for knee joint component fixation.²⁶⁾ Resolving the aseptic loosening of knee joint prostheses is an important part of the design of artificial knee joints.²⁸⁾

Instability was the second and third most common reason for failure described in the second and third report respectively. Instability can arise from an imbalance between the array and soft tissue. Owing to advancements made in surgical techniques, the percentage of instability-associated failures decreased in the 2012 report compared to the 2002 report. To reduce the incidence of instability-associated failure, stability should be ensured by accurate preoperative measurements on the one hand, and posterior stabilization of prostheses on the other.²⁶⁾²⁷⁾

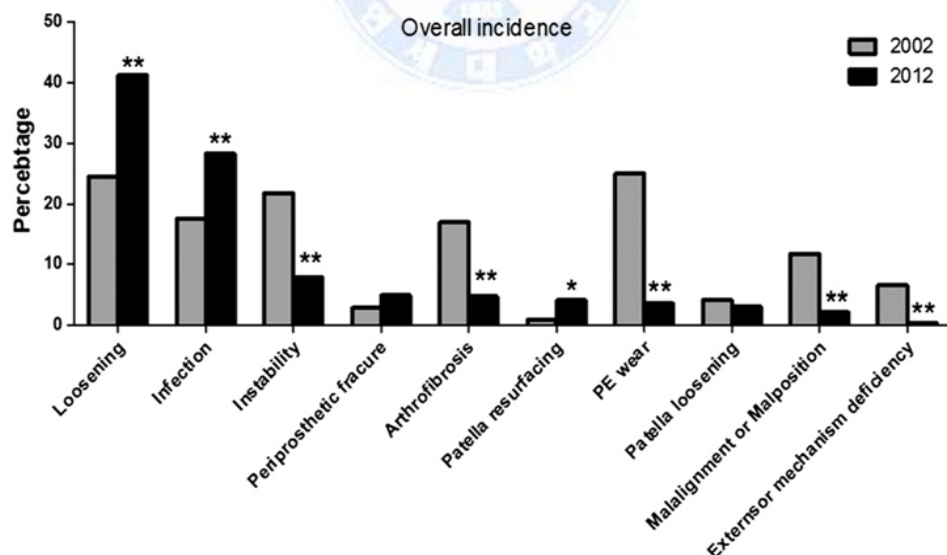


Fig. 16. Overall incidences in total knee arthroplasty in 2002 and 2012 ²⁷⁾

4. Revision Total Knee Arthroplasty

As described in section 3.3, satisfactory surgical outcomes from TKA and the high survival rates of replacement implants were verified in many reports and clinical outcomes. However, continuously repeating flexion and extension motions of the knee joint trigger the wear of the tibial insert, and the difference in elastic modulus between the bone and prosthetic material gives rise to the stress-shielding phenomenon, which results in bone loss and loosening of the bone–implant bond.¹⁹⁾²⁰⁾ Additionally, instability occurs due to the deviation of the alignment axis along which the implants are placed and thus results in loosening and fracture failure of the primary TKA.²²⁾²⁴⁾²⁵⁾²⁹⁾³⁰⁾ (Fig. 17)

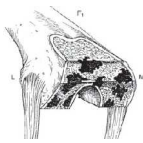
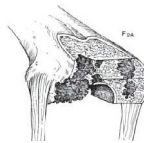
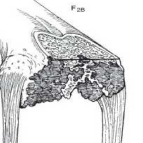
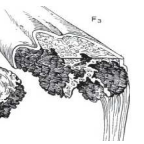

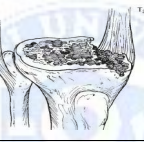
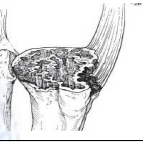



Fig. 17. The failure reasons in the total knee arthroplasty

Such failure of primary TKA requires the removal of the original implant and insertion of a new one. The removal of the primary artificial knee joint involves bone loss because a considerable part of the remaining natural knee joint components is removed together with the inserted replacement. (Table. 1.) A

revision TKR prosthesis is designed on the basis of worse bone conditions than those in the primary TKA and takes into account mechanical design elements to ensure better stability and articular function.³¹⁾³²⁾

Table 1. The classification of bone loss after the removal of total knee arthroplasty(Anderson Orthopedic Research Institute : AORI)

	Class I	Class II(A)	Class II(B)	Class III
Femur				
Tibia				

4.1 Necessity of revision total knee replacement prosthesis development

As of 2012, the global TKR prosthesis market size amounts to \$7.2 billion, with an average annual growth of 3.5%. The main causes for this rapid growth are the increasing incidence of osteoarthritis due to an increasingly aging population and the increasing obesity prevalence.³³⁾(Fig. 18) An even greater market increase is expected, given the growing demand for TKR due to leisure and sport activities of the younger population and the demand for revision TKR subsequent to primary TKR.

The current market share of revision TKR prostheses is lower than 10% of the entire knee prosthesis market, and the three largest global companies (Zimmer, DePuy, and Stryker) account for over 65% of the knee replacement market.³³⁾

The Korean knee replacement market size was 70.2 billion won as of 2012, with an average annual growth of 8%.³⁴⁾ Although two domestic companies have

developed primary TKR products and have succeeded in commercializing them, products from the leading global companies are still dominant in the domestic market; revision TKR products have not yet been developed domestically and the entire demand is met by imported devices.(Fig. 19)

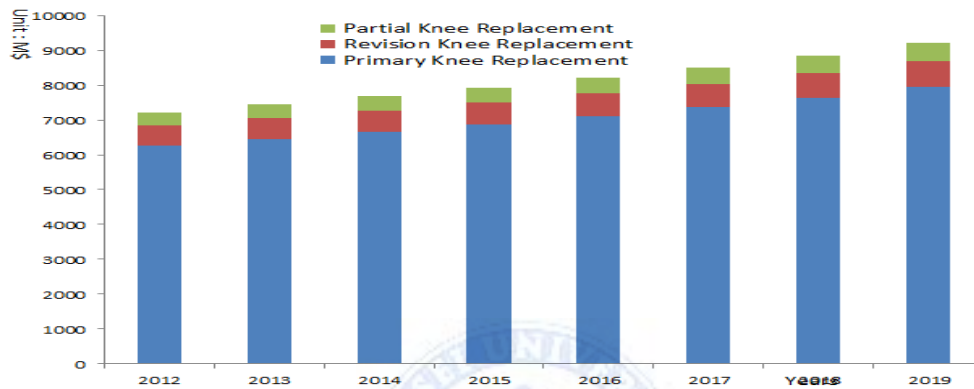


Fig 18. The global market forecast to 2019 in total knee replacement



Fig. 19. The Korea market forecast in total knee replacement³⁴⁾

5. Outline of This Research

Knee replacement research and development requires enormous time and investment from design to industrialization for evaluation and validation due to the high safety and reliability required for long-term implants in the human body.

Currently, the supply of revision TKR prostheses in Korea depends entirely on imported products. Against this background, the current study was conceived for the purpose of developing a new revision TKR prosthesis by establishing a system to meet the design components and clinical and mechanical requirements and performing evaluations and various tests on prosthetic materials for existing revision TKR prostheses. The newly developed prototype underwent all necessary tests and evaluations to meet the standards required for it for field application and industrialization. In particular, its mechanical stability and biological safety are two major factors to be considered because it is inserted into the human body and exposed to continuous loads and movements. For its biomechanical stability testing, analyses of structural strength, stress/strain, fatigue load characteristics, bond strength, and disassembly torque was performed using the finite element method (FEM). Its biological stability was tested in safety studies associated with toxicity, subcutaneous (intradermal) reactivity, and sensitization and corresponding tests. The feasibility of the new revision TKR prosthesis was determined according to the comprehensive analysis results of these tests and evaluations.

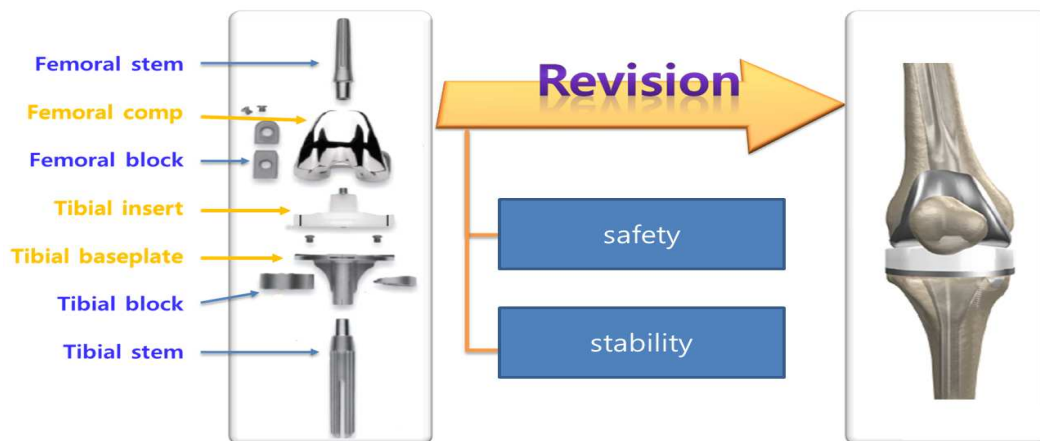


Fig. 20. The design concepts in a new revision total hip replacement.

CHAPTER II. Design element analysis and design of a revision total knee replacement prosthesis

1. Design Element Analysis and Design According to the Clinical Requirements

With the purpose of developing a new revision TKR prosthesis, design factors for a revision artificial knee joint to replace the primary TKR prosthesis, such as safety, stability, and modularity, were analyzed based on the commercialized primary TKR prostheses. The analysis results were applied to the design of the revision prosthesis, and the safety of the revision artificial knee joint thus designed was evaluated by performing safety testing for each structural component.

1.1 Stability

Considering the age-related limited activity level of most users of revision TKR prostheses, setting a high activity level for revision TKR may have undesirable effects of causing excessive motion that puts the weakened knees of the patients at higher risk of damage and injury. Therefore, a design that avoids a large medial and lateral rotation range and deep flexion and increasing stability is necessary.

One of the clinical requirements for primary TKR is maintaining the patient's movement abilities, taking into account situations requiring deep knee flexion, a large range of varus-valgus angle, and a large range of the contact-area internal rotation in flexion. However, in designing a revision TKR prosthesis taking into account clinical requirements, design parameters should have limited degrees of freedom. In this study design, parameters were configured at maximum flexion of 130°, varus-valgus angle of 2°, and contact-area angle in flexion of 4° (Fig. 21).

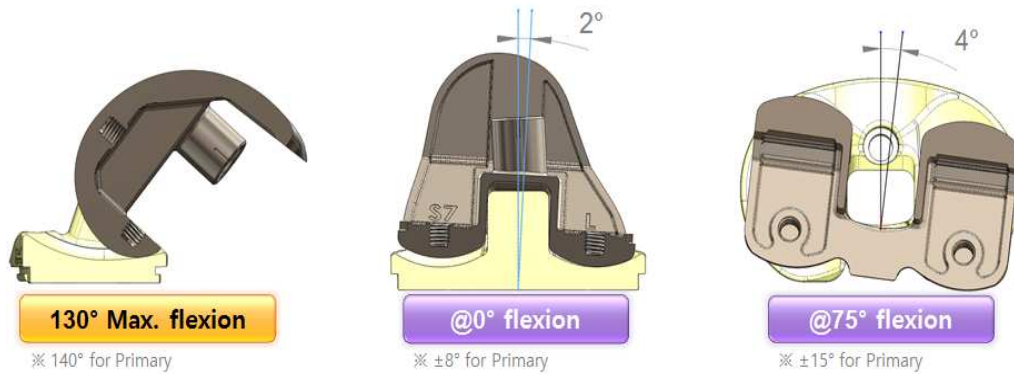


Fig. 21. The design parameters in range of motion of new R-TKR

Conformity was enhanced by increasing the anterior/posterior radius with respect to the sulcus point and matching the curvature of the femoral component in the coronal plane (Fig. 22). This structural design was considered optimal for increasing the contact area of the knee replacement and lowering the contact pressure, which contributes to preventing wear and damage of the artificial knee joint and enhancing stability by preventing dislocation.

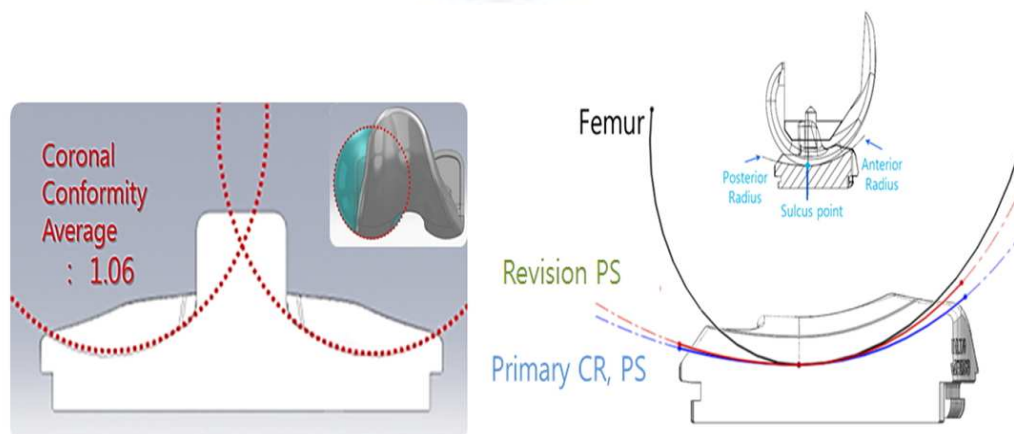


Fig. 22. The design parameters in conformity with femoral component and tibial insert of new R-TKR

1.2 Modularity

To stabilize the femur and tibia of patients with weakened bone qualities, a revision artificial knee joint should be additionally strengthened by replacing the damaged bone or providing structural augmentation. Stem extension is necessary to ensure sufficient bond strength when inserting the revision artificial knee joint into the bone with reduced bone mass due to the bone removed while removing the primary artificial knee joint. Additional fixation stability is ensured by deep insertion into the distal femur and proximal tibia when anchoring the prosthesis onto the femoral component and tibial baseplate.³⁵⁾³⁶⁾

The insertion points of the stem extension should be positioned at 35% from the femoral and tibial anterior borders so that they can be aligned with the tibiofemoral mechanical axis. (Fig. 23).

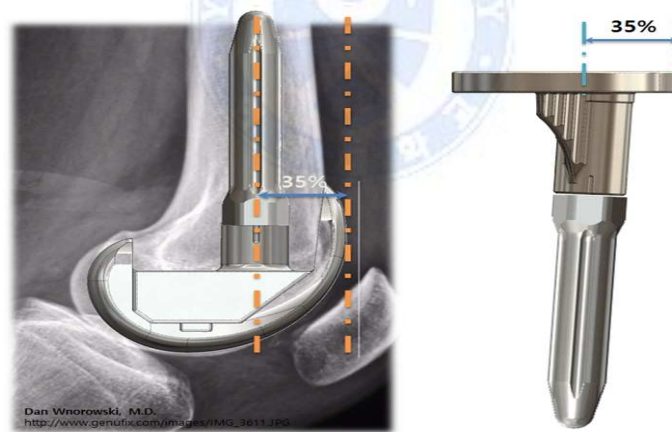


Fig. 23. The design parameters in stem extension

The stem housing connected to the femoral component should be configured to have an angle of 6° from the femoral shaft so that it can be inserted parallel to the mechanical axis. The stem extension attaching to the tibial baseplate should be

configured to be positioned within the cancellous bone without contacting the cortical bone, taking into account the posterior slope of 3° . The offset adapter should be designed to allow flexible insertion of the stem extension, taking into account different anatomical shapes according to the indication for the revision TKR, as well as varying degrees of resection of damaged bone surfaces and insertion points. An offset adapter should be designed to allow offset at 2-, 4-, and 6-mm intervals, thus personalizing the prosthesis to the individual anatomic characteristics depending on the indication for the revision TKR (Fig. 24).

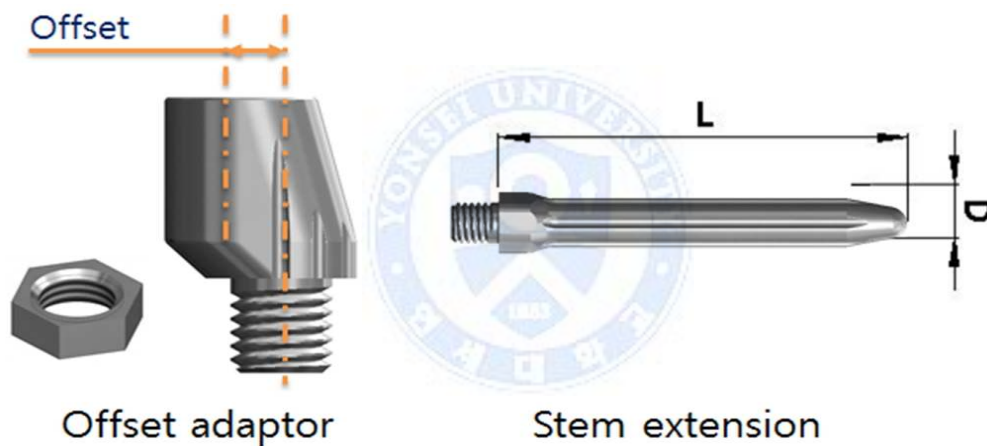


Fig. 24. The design parameters in Stem extension and offset adaptor

Bone loss arising from femoral and tibial component loosening and osteoporosis mostly occurs in the knee replacement areas. Therefore, bony defects should be addressed during revision TKR surgery with augmentation blocks. Since bone loss regions vary according to the indication for revision TKR, augmentation blocks connected with the femoral component should match the anterior, posterior, or distal aspect of femur. The tibial baseplate should be designed for two types:

overall augmentation of a certain thickness of the proximal tibia and partial (medial or lateral) augmentation. The thickness of the newly designed prosthesis was configured at 5 and 10 mm to be applied according to the extent of bone loss, and the design was laid out to be equally usable for lateral and medial augmentation. For the fixation to the femoral component and tibial baseplate, bone cement or bolts can be used. When fixing with bone cement, a 0.8-mm cement pocket should be designed to enable placement on the exact position (Fig. 25). An augmentation block should be designed to have an adequate thickness to compensate for the bone loss, and wedge-type augmentation is considered desirable in reducing the size difference between the revision TKR and the proximal tibia depending on the degree of bone resection.

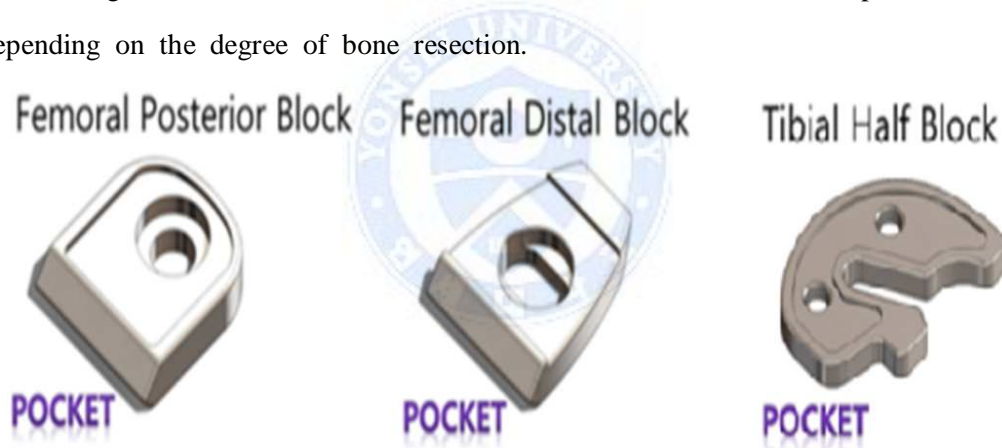


Fig. 25. The design parameters in femur & tibia blocks for bone deficit

1.3. Safety

The major mechanical functions of a revision artificial knee joint are equivalent to those of the primary artificial knee joint, but attention should be paid to the fact that patients' excessive activity and exercise can trigger dislocation, failure, or instability of a revision artificial knee joint. Safety-minded design is especially

important for revision TKR prostheses because patients with revision implants are in aggravated clinical and biomechanical conditions compared to the conditions at the time of their primary TKA.

Dislocation during flexion can be prevented by designing the tibial insert post of the revision artificial knee joint to contact the femoral component directly. The insert post is designed to have a concave shape, which reduces stress in the contact area and implements rollback. Additionally, it should increase the jump distance for estimating flexion-induced dislocation. Jump distance is defined as the perpendicular distance needed for the femoral cam to ride over to the tibial post in a posterior-stabilized (PS)-type knee prosthesis (Fig. 26). It is desirable for the femoral cam to move inferiorly after contacting the tibial post as the knee flexion angle increases. This feature is considered especially important for a deep-flexion knee prosthesis.



Fig. 26. The design parameters in jump distance and rollback between femur & inerts components

Among the parts of the tibial component of an artificial knee joint, the baseplate and insert are the parts carrying the risk of dislocation, and for safety enhancement of revision TKR, it is recommended to fix these two parts. Combining the metal locking rod running from the anterior insert post through the baseplate can prevent the dislocation of the insert during flexion and extension. The insert locking rod was thus designed to facilitate connection with the insert by tapping without an extra connection part and to prevent postoperative disassembly.

The stem extension is another part connected to the baseplate for the same reason as the locking rod. The screw method is used to connect these two parts. This method has the disadvantage that once the initial spiral compression is relaxed, the joined parts are gradually disassembled only by a small external force. This problem can be solved by enhancing the bond strength of the two parts by equally distributing the force exerted from outside with a spiral lock system (Fig. 27). It is an important design feature of revision TKR to ensure stable linkages between component parts with respect to the torque induced by medial-lateral rotation and repeated load. In thread design, it is important to form a wedge so that constant loading can be distributed over the contact surface of the spiral lock nut by matching the thread size of the stem extension.

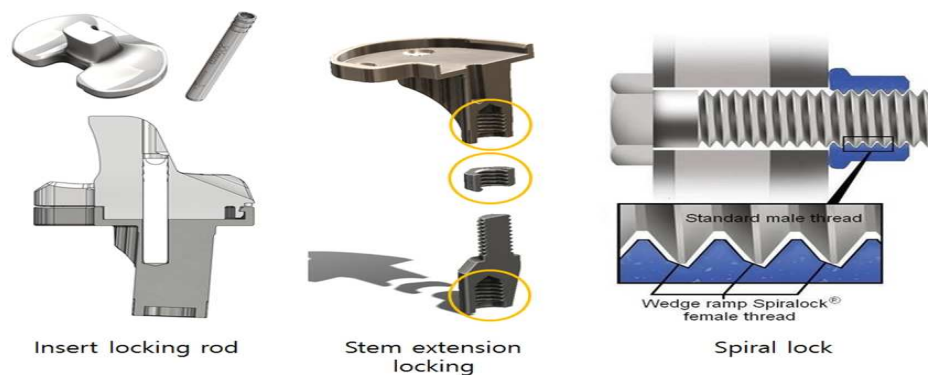


Fig. 27. The design parameters in insert locking rod and spiral lock system

2. Structural Stability Evaluation of the Revision Knee Replacement Prosthesis by Component Part

The performance features of the proposed revision TKR were evaluated with a variety of tests. Structural stability is a key factor by the inherent nature of the knee joint. Structural stability and the stability of each connector were validated using the finite element analysis (FEA) method.

2.1. Structural stability of each revision TKR component

The comparative mechanical strength testing is performed on the primary and revision artificial knee joints using finite element analysis (FEA) in order to test the safety of each component of the revision TKR constructed with new design parameters.

Structural stability of each components were validated using the finite element analysis(FEA) method. The Structural stability test was conducted using finite element analysis(ABAQUS v6.10) and performed ASTM F1223-08³⁷⁾ and F1800-12³⁸⁾ and compared with primary TKR system.

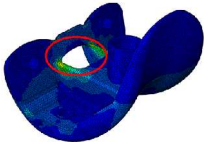
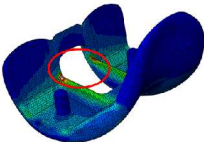
2.1.1 Method for structural stability testing for each component

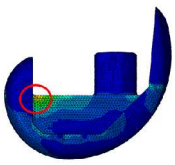
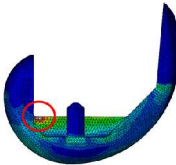
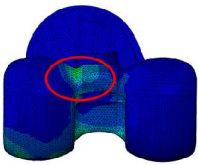
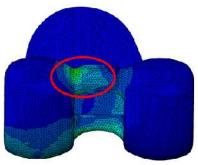
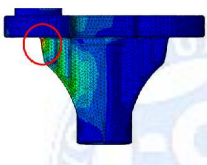
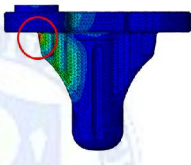
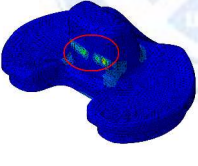
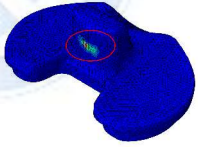
The test method and load constraint conditions were chosen in compliance with the ASTM specification for conducting the mechanical strength test of a TKR as the international standard test method. Specifically, the wedge test and eccentric test (ASTM F1223-08) were performed on the femoral component, the eccentric test(ASTM F1800-12) on the tibial baseplate, and the post-cam strength test on the tibial insert(Table 2). Additionally, load and constraint conditions were applied in the testing using ABAQUS6.10(Dassault Systems,Massachusetts,USA).

2.1.2 Result analysis and interpretation

The dynamic stabilities of the primary and revision artificial knee joints were compared by measuring the stress distribution and the von Mises stress (VMS) (Table 3). The strength test revealed that the femoral component of the revision TKR prosthesis was strengthened by over 30% compared to the primary TKR prosthesis, presumably with the intent of preventing a decrease in strength when increasing the height of the PS box to prevent dislocation. In the eccentric test on the tibial baseplate, the revision TKR prosthesis exhibited about 23% lower resistance than the primary type. This is assumed to be attributable to the hole created when bolt-fixing the reconstruction part of the revision artificial knee joint to the tibial baseplate. Nevertheless, given the yield stress of cobalt-chrome (CoCr), the tibial baseplate material, and body weight, sufficient structural stability can be considered secured when inserted into the body. The revision-type tibial insert was verified to have about 30% higher strength than the primary type, thus demonstrating that the design values giving priority to stability and strength of the tibial insert post were adequately reflected.

Table. 3. The results in stress distribution in component of new R-TKR

Test	Stress Distribution		VMS [MPa]	
	Revision	Primary	Revision	Primary
Wedge test (ASTM F1223-08)			1055.37	1651.23

Compression test (ASTM F1223-08)			604.2	965.1
Eccentric test (ASTM F1223-08)			1250.31	1273.48
Eccentric test (ASTM F1800-07)			406.9	330
Post-cam Strength test			22.92	32.05

2.2 Bond strength test of the revision knee replacement prosthesis

The extended stem and its stable fixation to the femoral component and tibial baseplate are important revision artificial knee joint design features in terms of safety. It is more solicited than the tibia in playing the function of stress transmission and fixation. The stability of the revision TKA prosthesis was evaluated with FEA after measuring the bond strengths of the individual components and combined parts, including the extended stem.

2.2.1 Connector bond strength test method

FEMs were created for the femoral component and tibial baseplate combined with the extended stem using the same-size extended stem. Mimicking the shape of the components when inserted into the knee, the tibial baseplate was configured to have a fixed extension stem lower-end displacement as a boundary condition, and the stress at the connector was measured under the load of an 8-fold heavier body weight. For the femoral component, its condyle connected with the tibial insert was fixed, and an 8-fold heavier body weight was applied to the proximal aspect of the extension stem (Fig 28).

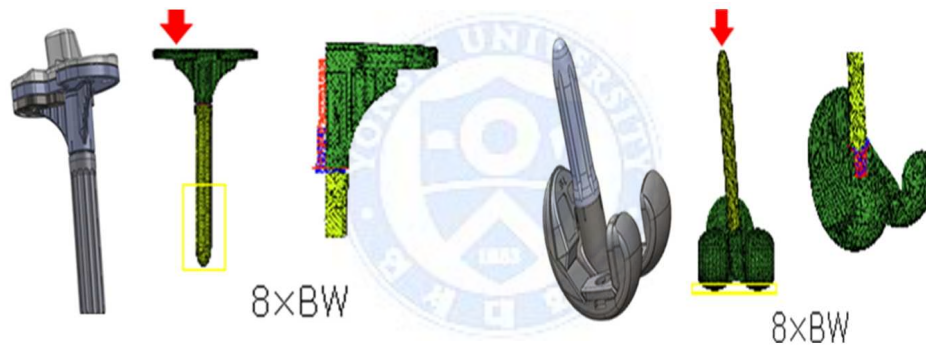


Fig. 28. The test methods including loading condition for structural combination stability in femur and tibia component with extension stem

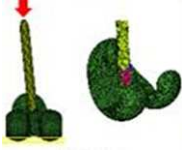



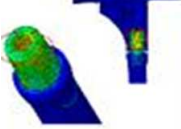

2.2.2 Bond strength analysis of the connector of the extended stem and each component

The connector between the tibial baseplate and the extended stem exhibited a peaked VMS (PVMS) of 1305.17 MPa, whereby the stress was transferred to the lower end of the stem. In line with the design of the tibial insert slope, the stem was inserted at a 3° angle; as a result, a stress of 180 MPa was measured on the

side medial to the stem connector.

A PVMS of 504.7 MPa was measured on the connector between the femoral component and the stem, with the stress distributed downward to the lower end of the connector. Additionally, VMS was measured medially to the connector due to the moment generated by a stem insertion slope of 6° parallel to the femoral insertion axis angle. Even though high stress was generated at the connector of the connection model, considering the severe-case FEA test condition of an 8-fold heavier body weight, these measured values are considered to reflect that the revision TKR prosthesis design features have been superior in taking stability and bond strength into account.

Table. 4. The results in stress distribution in femur and tibia united extended stem FE model

Components	Loding Condition	Stress distribution		VMS(MPa)
Femur parts	 8×BW			504
Tibial parts	 8×BW			1305

CHAPTER III. BIOMECHANICAL STABILITY EVALUATION ON THE REVISION TOTAL KNEE REPLACEMENT PROSTHESIS

A main difference between primary and revision TKR users is that the latter are older than the former. This should be reflected in the revision TKR prosthesis design. Additionally, various primary TKA failure mechanisms should be taken into consideration, and related problems should be resolved. Therefore, a mechanical stability test will be performed to ensure the stability of the proposed revision TKR prosthesis. Furthermore, its biomechanical stability will be verified by developing a surgical model and analyzing the actual in vivo behavior and performance of the proposed revision TKR prosthesis in terms of load transmission and stress transfer.

1. Evaluation of the Mechanical Stability of the Proposed Revision Total Knee Replacement Prosthesis

1.1 Baseplate fatigue test (ASTM F1800-12)

The knee joint is exposed to a constant load by daily activities, such as standing and walking, and fracture of the artificial knee joint due to concentrated load is one of the main reasons for revision TKA. Therefore, among the components of the revision TKR prosthesis, fatigue load-related dynamic characteristics of the tibia baseplate will be analyzed.³⁸⁾

1.1.1 Baseplate fatigue test method

The durability of the tibial baseplate was tested with the fatigue test in compliance with ASTM F1800-12.³⁸⁾ The tibial baseplate was fixed, and the prepared specimen was fixed to the other side with epoxy resin adhesive using the tibial insert material. Fatigue testing began by applying test vibration according to the test specification ($\leq 30\text{Hz}$) and test load, and it continued until the 1×10^7 cycle as reached or the tibial baseplate sustained crack or fracture (Fig. 29). The fatigue-test experimental conditions and fatigue load conditions are presented in Tables 5 and 6 respectively.

The fatigue load test was conducted on six tibial baseplates prepared as test specimens. In accordance with the ASTM test method, load level 1 (90N–900N; 10,000,000 cycle) was applied to specimen 1. Based on the test result of specimen 1, fatigue load level 8 was applied to specimens 2 through 6 at 10×10^6 cycles, and the changes in the specimens were observed.

Table. 5. The fatigue test methods according to ASTM 1800-12

Maximum load	<ul style="list-style-type: none">• 90N to 900N. followed by progressive loading for specimen 1.1• 440N to 4,400N for specimen 1.2 to 1.6
Ration R	<ul style="list-style-type: none">• 10
Dynamic loading wareform	<ul style="list-style-type: none">• sinusoidal
number of run-out cycles	<ul style="list-style-type: none">• 10,000,000 cycles
Test environment	<ul style="list-style-type: none">• dry at ambient air
Temperature	<ul style="list-style-type: none">• Room condition
Embedding medium	<ul style="list-style-type: none">• filled epoxy casting resin
Spacer for load application	<ul style="list-style-type: none">• 13.0mm diameter \times 6mm aluminum spacer
Load application	<ul style="list-style-type: none">• a metal ball combined with a ball bearing

Table. 6. Progressive fatigue loading for specimen 1.1

Load level	Min. Load [N]	Max. Load [N]	Cycle
1	90	900	10,000,000
2	140	1,400	1,000,000
3	190	1,900	1,000,000
4	240	2,400	1,000,000
5	290	2,900	1,000,000
6	340	3,400	1,000,000
7	290	3,900	1,000,000
8	440	4,400	1,000,000
9	490	4,900	1,000,000

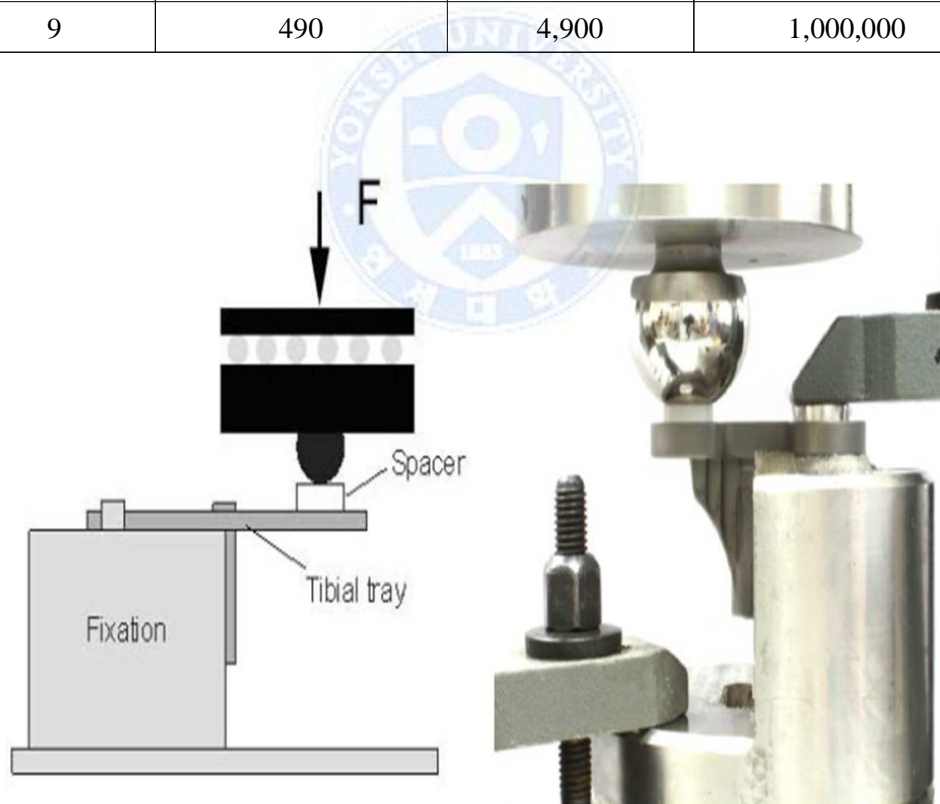


Fig. 29. The fatigue testing with tibial baseplate according ASTM F 1800-12

1.1.2 Baseplate fatigue test results

Based on the result of the fatigue load test on specimen 1, the test was discontinued at 3605 cycles at load level 9. According to the conditions described in Table 7, fatigue load was gradually increased for each load level. The test was discontinued at 17,003,605 cycles because of specimen loosening at the fixed part bonded with epoxy resin. The minimum and maximum displacements at the end of the test were 0.5mm and 0.8mm (difference: ~ 0.2mm) (Fig. 31), and micro-fine deformation was observed on the baseplate at the part directly exposed to load (Fig. 30). Microscopic examination of the specimen did not show any cracked or fractured part.

Table 7. Results for specimen 1 (tested by progressive loading)

Load level	Min. Load [N]	Max. Load [N]	Cycle	Result
1	90	900	10,000,000	No Failure
2	140	1,400	1,000,000	No Failure
3	190	1,900	1,000,000	No Failure
4	240	2,400	1,000,000	No Failure
5	290	2,900	1,000,000	No Failure
6	340	3,400	1,000,000	No Failure
7	290	3,900	1,000,000	No Failure
8	440	4,400	1,000,000	No Failure
9	490	4,900	1,000,000	Loosening from the embedding occurs



Fig. 30. A slight plastic deformation of specimen 1.1 after 3605 load cycles³ at load level 9

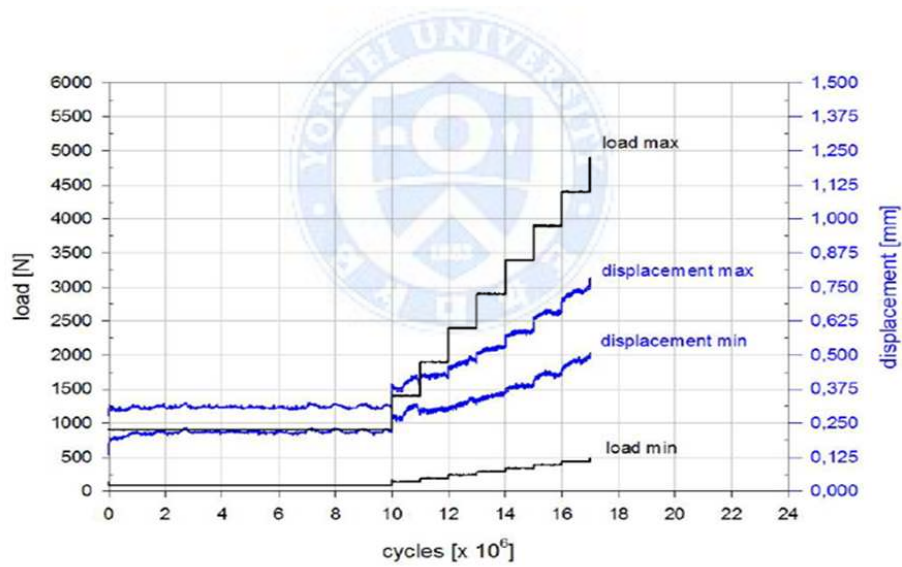


Fig. 31. Load and displacement(min/max) curves by number of loading-specimen 1

From the test result on specimen 1, 4,900N was found to be the upper fatigue load limit for the material clamping the specimen, which excluded load level 9. Therefore, load level 8 was chosen as the load to be applied to the specimens to

evaluate their fatigue load characteristics. The test was conducted under more severe conditions than the 900N at 10^6 cycles as specified in the ASTM guide line in order to secure mechanical stability against design fatigue load. Specimens 2–6 were subjected to test loads and frequencies exceeding the specified values by 4.9- and 10-fold , respectively. In the inspection of specimens 2–6 after the load application at 10^7 cycles, neither fracture nor permanent deformation was found. Fatigue load is an essential design feature determinant for the service life and stability of the artificial knee joint because of the steady knee replacement due to its steady exposure to load. The proposed revision TKR prosthesis, designed on the basis of the results o f the fatigue load test, which was performed in this experiment under higher fatigue load conditions than the international test standard, exhibits sufficient stability against fatigue load, thus proving its adequacy for application as a long-term knee implant.

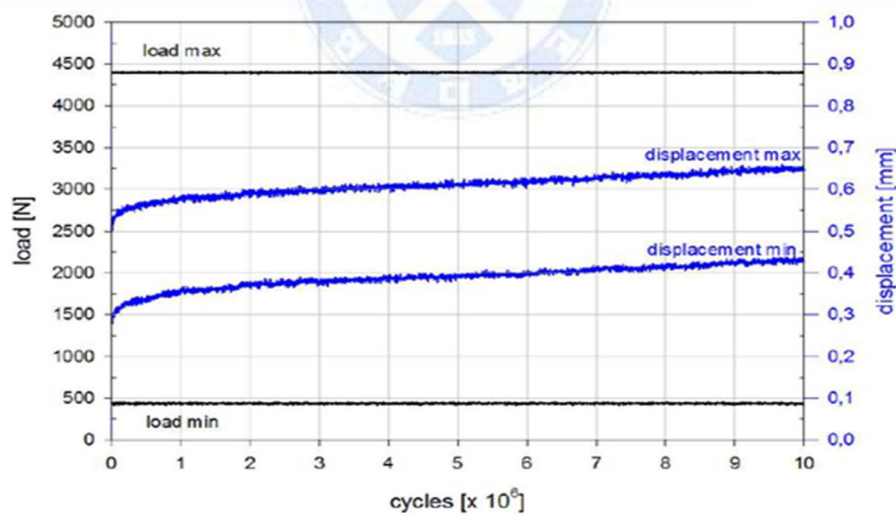


Fig. 32. Representative graphs for load and displacement(min/max) by number of loading cycles - specimen 2

1.2 Stem extension assembly locking test (ASTM F1814-97a)

Tests on modularity and safety should be performed on combined parts of the revision TKR prosthesis to evaluate bond strength by measuring assembly and disassembly torques. This section describes the test procedure (ASTM F1814-97a) and results regarding the assembly safety and disassembly convenience of the stem extension and offset adaptor.³⁹⁾

1.2.1 Assembly locking test method

Using the bolt output test with machine from SCHATZ, the test joint components were assembled at tightening torques of 9.5, 11.5, 13.5, and 15.5 Nm, and the disassembly-inducing loading and the extent of damage to the screw shape were measured. It was checked whether the applied assembly torque and disassembly torque matched and whether the disassembled bolts remained intact. The assembly locking test was performed 8 times per specimen at a rotating speed of 4 rpm (Fig. 33) using a jig designed to apply torque to the extension and offset adaptor parts. Subsequently, visual inspection was performed to see whether the bolts sustained damage (Fig. 34).

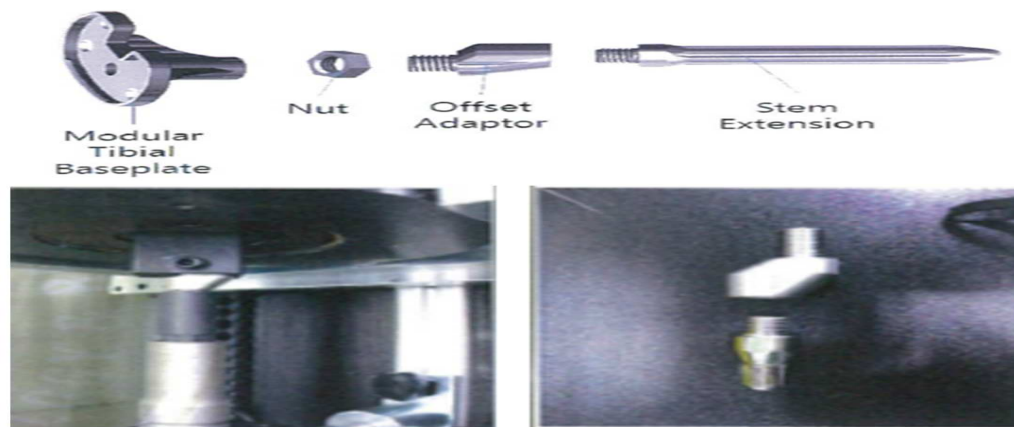


Fig. 33. The assembly/disassembly locking test with offset adaptor and stem extension

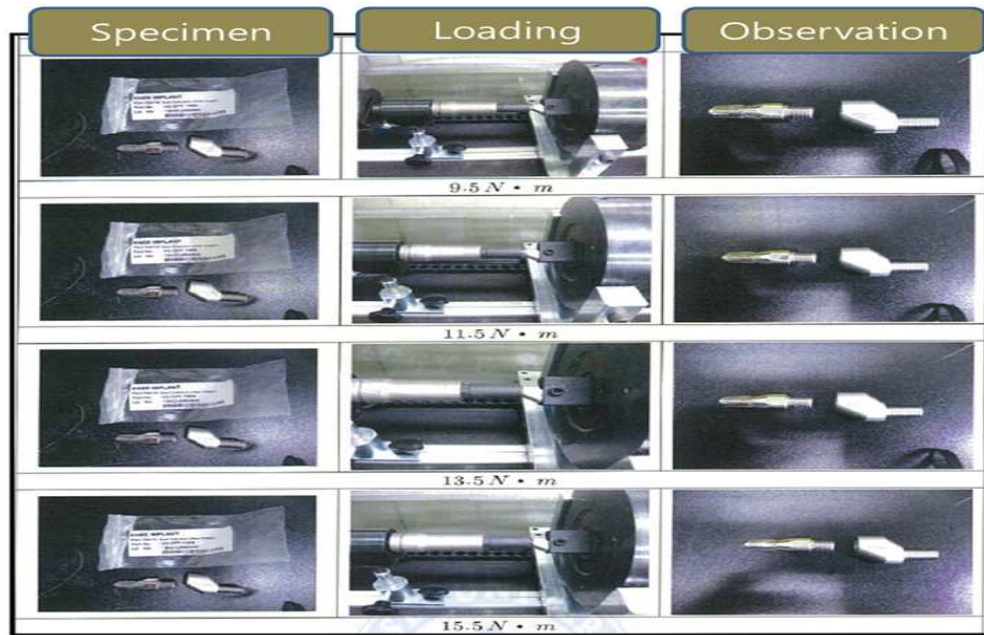


Fig. 34. The measurement of assembly and disassembly torques with SCHATZ machine

1.2.2 Assembly locking test results

The stem extension assembly locking test was conducted and the assembly and disassembly torques were measured for each tightening torque in order to calculate the assembly-to-disassembly torque ratio. Each specimen was subjected to 8 test runs at 9.5, 11.5, 13.5, and 15.5 Nm, which resulted in ratios ranging from 99.7% to 101%. The overall average of all individual test results was 100.5% (Table 8). This is superior performance compared to normal bolts, considering that bolts generally have assembly-to-disassembly torque ratio of ~90%, demonstrating that greater torque than the assembly torque is necessary to loosen the bolts used for connecting the parts of the extension stem and offset adaptor. No deformation of the bolts observed. These results show that stability against stem extension loosening has been secured.

Table. 8. The result of assembly locking tests

Loading Condition		Assembly Torque(N.m)	Disassembly Torque(N.m)	D.T/A.T(%)
9.5 N·m	1	9.53	9.47	99.4
	2	9.51	9.36	98.4
	3	9.51	9.12	95.9
	4	9.52	9.40	98.7
	5	9.50	9.57	100.7
	6	9.52	9.70	101.9
	7	9.52	10.18	106.9
	8	9.50	9.09	95.7
11.5 N·m	1	11.54	11.44	99.1
	2	11.53	11.21	97.2
	3	11.53	11.48	99.6
	4	11.51	11.49	99.8
	5	11.5	11.69	101.7
	6	11.55	11.50	99.6
	7	11.51	12.10	105.1
	8	11.51	11.50	99.9
13.5 N·m	1	13.50	12.98	96.1
	2	13.51	13.53	100.1
	3	13.51	13.86	102.6
	4	13.51	13.67	101.2
	5	13.50	13.93	103.2
	6	13.53	13.56	100.2
	7	13.52	14.24	105.3
	8	13.52	13.52	100.0
15.5 N·m	1	15.51	14.79	95.4
	2	15.52	15.73	101.4
	3	15.51	16.12	103.9
	4	15.53	15.75	101.4
	5	15.53	16.00	103.0
	6	15.51	15.55	100.3
	7	15.53	16.05	103.3
	8	15.55	15.67	100.8

2. Finite Element Modeling and Biomechanical Analysis of Surgical Outcomes

A FEM-based surgical model with the revision artificial knee joint inserted (hereafter referred to as the “implant model”) was implemented with the intent to evaluate the durability and safety of the proposed revision TKR prosthesis by analyzing its biomechanical behavior and performance. Biomechanical analysis is an essential part of TKR prosthesis evaluation, given the fact that excessive load concentration can cause its fracture⁴⁰⁾ and trigger abnormal load transfer between the artificial knee joint and bone, which can result in substantial deformations in the adjacent parts or the implant, thus affecting the initial stability of the revision TKR.²⁹⁾³⁰⁾ For this reason, a FEM for the human body with the tibia of the revision TKR prosthesis inserted was created and simulations were performed to evaluate the structural stability of the revision artificial knee joint tibia and its adjacent structures. Additionally, load distribution and strain on the proximal and distal aspects of the tibia were analyzed to evaluate the biomechanical stability of the proposed revision TKR prosthesis.

2.1 Revision TKR finite element model creation

The researcher developed a 3D tibial reconstruction model for FEA from computed tomography (CT) images of a patient diagnosed with degenerative arthritis, using Mimics 14.0 software (Materialize, Leuven, Belgium), as a preparation for creating the implant model. This FEM comprises 104,876 nodes and 454,165 elements, on which material properties were applied to their respective anatomical areas, as outlined in⁴¹⁾⁴²⁾⁴³⁾⁴⁴⁾⁴⁵⁾(Fig.35, Table 9).

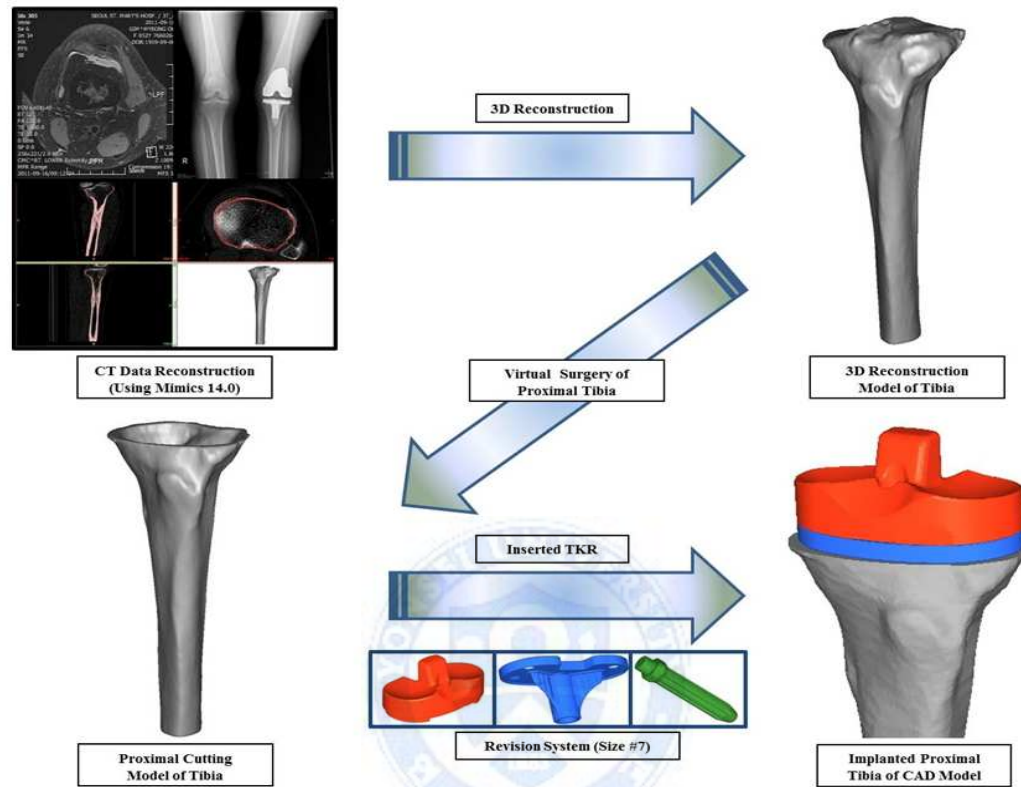


Fig. 35. Patient's tibia geometry and insertion R-TKR within tibia

Table. 9. Mechanical properties for finite element model⁽⁴¹⁾⁽⁴²⁾⁽⁴³⁾⁽⁴⁴⁾⁽⁴⁵⁾

Component	Elastic Modulus [MPa]	Poisson's Ratio	Yield Strength [MPa]
Cortical Bone	17,000	0.3	114
Cancellous Bone	300	0.3	15
Spacer (UHMWPE)	1,000	0.46	21
Baseplate (CoCr)	200,000	0.3	450
Stem (Ti Alloy)	113,000	0.33	150

The implant model was created by inserting the proposed revision TKR prosthesis into the knee following the same procedure as in a real-life revision TKA. After fixing the parts along the mechanical axis, the implant model was completed by adjusting the tibia through the alignment of the varus and posterior slope with 2.0° and 3.0° tibial rotation, respectively, lest the extended stem with the tibial baseplate of the revision TKR prosthesis should protrude outside the tibia.⁴⁶⁾ For the fixation conditions, in simulation of the use of bone cement, general contact conditions were applied using ABAQUS 6.10 (Dassault Systems, Massachusetts, USA) for the configuration of the contact conditions between the revision TKR prosthesis's tibial component and the insertion part of the tibia. An FEM mimicking the bone cement was implemented for the contact area between the tibia and the revision TKR prosthesis's tibial component in order to model bone cement conditions for the fixation of the revision artificial knee joint's tibial component(Fig.36).

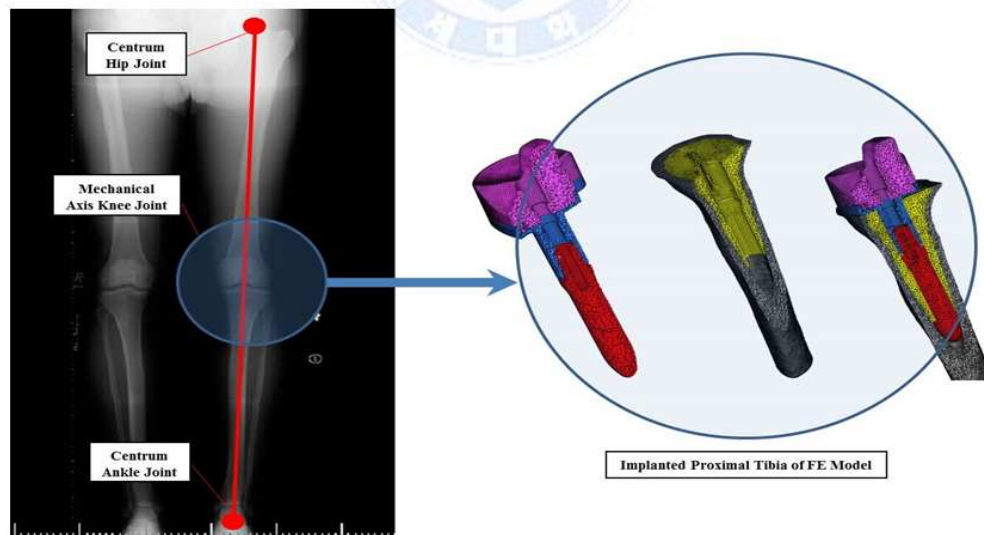


Fig. 36. Surgical FE models according to right location within tibia geometry

The load condition applied to the FEM was configured to be 2000N, which is equivalent to a 3-fold heavier body weight exerted perpendicularly on the tibial articular surface, to reflect the actual dynamic feature acting on the knee joint of an arthritis patient. Additionally, loading was applied perpendicularly to the tibial spacer's articular surface, and the load distribution ratio on the medial and lateral articular aspects was configured to be 6:4.⁴⁷⁾ The distal tibia was fixed by completely constraining the x-, y-, and z- direction translation of 20mm from the distal extremity of the tibia to the proximal tibia.(Fig. 37)

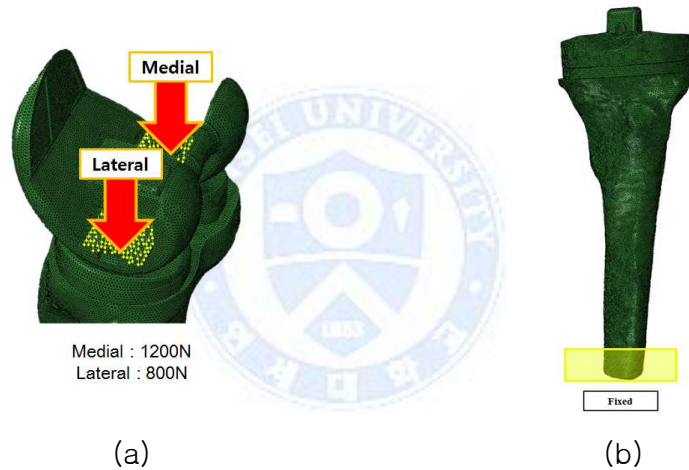


Fig. 37. (a)Loading Condition (2000N), (b)Fixed Condition (20mm)

Result analysis was preceded by the validation of the FEM. FEM validation was performed by comparing the strain generated on the tibia of the implant model with that measured in previous studies.⁴⁷⁾⁴⁸⁾ Furthermore, the PVMS on the tibial component of the revision TKR prosthesis, tibial cortical bone, and tibial cancellous bone was estimated for stability evaluation, and the resultant values were compared with the yield strength reflected in the safe factor ($N = 4.0$) of

each material. Based on the results, a structural safety analysis was performed on the tibial component of the revision TKR prosthesis as well as on the tibia with the inserted tibial component of the revision TKR prosthesis. Furthermore, changes in the stress/strain distribution characteristics of 8 regions of interest ($\varnothing 10$ mm) from the proximal tibia to the distal extremity of the tibia were analyzed in order to determine the influence that the tibial component of the revision TKR prosthesis inserted deep into the tibia has on the tibia.(Fig. 38) The analyzed changes were compared with the changes in the stress/strain distribution characteristics of a currently marketed product (Scorpio TS Revision System, Stryker Corp., MI, USA) for an effective and practical evaluation of the impact of the proposed revision TKR prosthesis on the tibia.

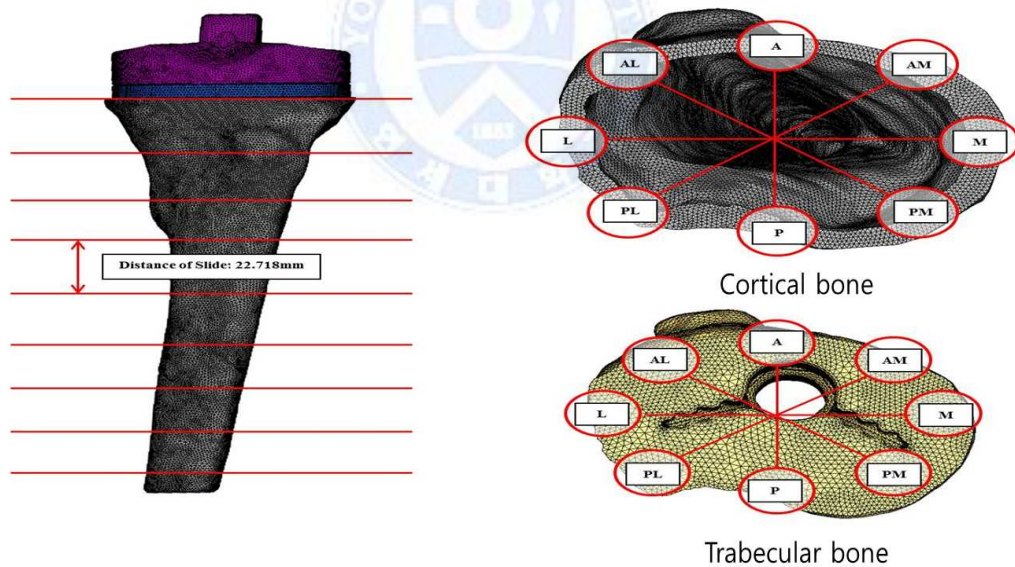


Fig. 38. The measurements of the stress and strain in tibia cortical and cancellous bone

2.2 The revision TKR prosthesis's biomechanical stability analysis results

For the evaluation of the biomechanical characteristics of the proposed revision TKR prosthesis, the validation of the implant model with an inserted tibia baseplate with stem extension was performed. As the validation method, strains were analyzed and the analytical values of the implant FEM model of the proposed TKR prosthesis and the measured values from previous studies were compared⁴⁸⁾, which yielded the finding that the micro strain values in the same measurement area were within the deviation range, thus demonstrating similarity (Fig. 39). Furthermore, the estimated distribution pattern on the proximal tibia of the implant model showed similarity to known patterns. With the mechanical properties of the implant model thus validated, biomechanical analysis was performed on the implant model.

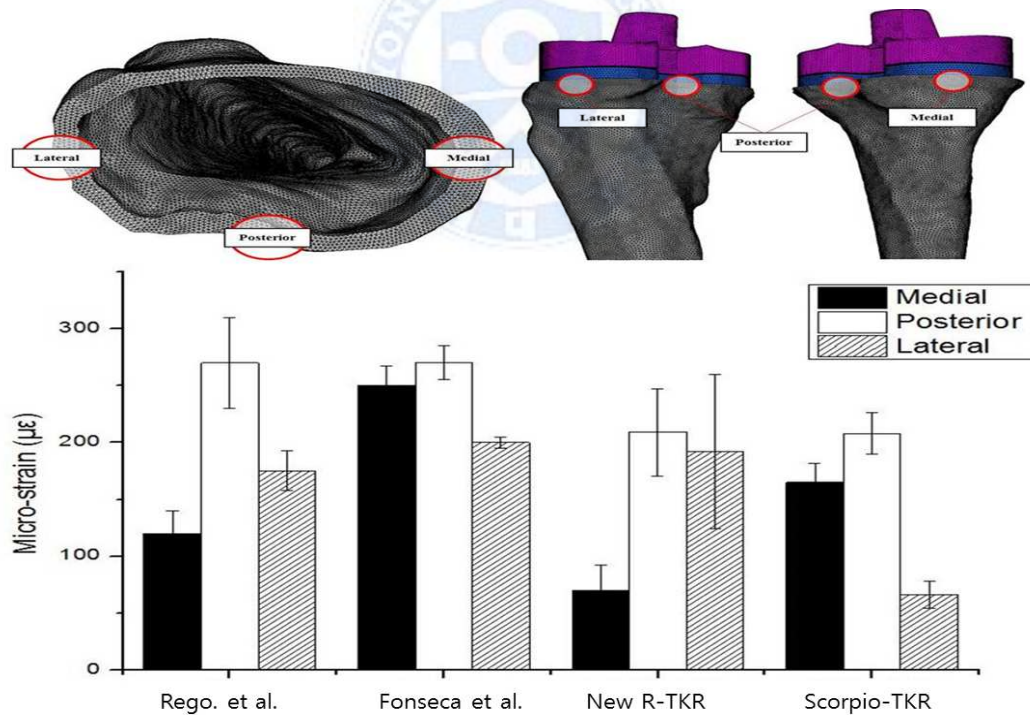


Fig. 39. Comparison of strain distribution within implanted proximal tibia

For the validation of the structural stability of the proposed revision TKR prosthesis, the PVMS of each component was examined. PVMS was observed at the upper extremity of the anterior insert part, which was verified to be equivalent to 0% with respect to the yield strength of ultra-high molecular weight polyethylene (5.25 MPa), taking the safety factor ($N = 4.0$) into account. On the tibial baseplate, the PVMS was exhibited in the posterior aspect of the connector of the extended stem, which was verified to be equivalent to 4% with respect to the yield strength of CoCr (112.5 MPa), taking the safety factor ($N = 4.0$) into account. For the extended stem inserted deep into the tibia, the PVMS was estimated at the connection with the baseplate, which was verified to be equivalent to ~8% with respect to the yield strength of Ti alloy (37.5 MPa), taking the safety factor ($N = 4.0$) into account. These values allow the assumption that products designed with the proposed revision TKR prosthesis would not pose problems of structural stability.

Insertion-related bone stability is also an important inspection item in revision TKA. The PVMS of the cortical bone (16.174 MPa) was estimated at the lateral aspect of the resection surface. This was verified to correspond to ~70% of the yield strength of the cortical bone (28.5 MPa), taking the safety factor ($N = 4.0$) into account. For the cancellous bone, a PVMS of 2.594 MPa was estimated at the posterior aspect, which was verified to correspond to ~70% of the yield strength of the cortical bone (3.75 MPa), taking the safety factor ($N = 4.0$) into account.

From these results of the safety analysis of the component parts of the tibial components of the proposed revision TKR prosthesis, structural stability can be assumed to be secured, so that no additional improvement or supplement is

necessary for the design elements from the stability-related point of view.

An additional analysis was performed on the tibial component of the proposed revision TKR prosthesis by comparing the stress/strain levels of the tibial cortical and cancellous bones with those of the control, a currently marketed product. On the cortical bone of the proposed revision TKR prosthesis, high stress/strain levels were verified at the proximal posterior part (3.56 ± 1.31 MPa / 209.4 ± 76.7 $\mu\epsilon$) and lateral part (6.04 ± 5.67 MPa / 192.4 ± 136.1 $\mu\epsilon$), with the level increasing at the anterior part (4.45 ± 0.06 MPa / 131.4 ± 37.7 $\mu\epsilon$) toward the distal extremity. In the control product, high stress/strain levels were verified at the proximal posterior part (2.93 ± 0.78 MPa / 208.82 ± 36.1 $\mu\epsilon$) and anterolateral part (3.73 ± 2.66 MPa / 225.23 ± 110.96 $\mu\epsilon$), with the level increasing at the anterolateral part (9.89 ± 1.58 MPa / 215.30 ± 12.2 $\mu\epsilon$) toward the distal extremity (Fig. 39).

On the cancellous bone of the proposed revision TKR prosthesis, high stress/strain levels were verified at the proximal posterior part (0.5 ± 0.51 MPa / 2086.13 ± 2403.1 $\mu\epsilon$), with the level increasing at the anterolateral part (0.2 ± 0.04 MPa / 484.54 ± 93.3 $\mu\epsilon$) toward the distal extremity. In the control prosthesis, high stress/strain levels were verified at the proximal posterior part (0.27 ± 0.09 MPa / 908.58 ± 163.03 $\mu\epsilon$), with the level increasing at the antero-middle part (0.72 ± 0.13 MPa / 1586.03 ± 327.54 $\mu\epsilon$) toward the distal extremity (Fig. 40).

The proposed revision TKR prosthesis and the control product had similar stress/strain distribution patterns. Specifically, the proximal tibia of the proposed revision TKR prosthesis had generally similar or higher strain compare to the control (cortical bone: higher by 61.89 ± 59.37 $\mu\epsilon$ on average; cancellous bone:

higher by $963.79 \pm 238.9 \mu\epsilon$ on average), and the closer to the distal tibia, the strain tended to be similar or lower compared to the control (cortical bone: lower by $67.36 \pm 12.5 \mu\epsilon$ on average; cancellous bone: lower by $893.88 \pm 455.17 \mu\epsilon$ on average). In other words, the proposed revision TKR prosthesis induced more load transfer in the proximal tibia and less load transfer in the distal tibia. This result implies that the proposed revision TKR prosthesis's tibial component can trigger the strain-shielding phenomenon in the proximal tibia despite the improvement compared to the control. In the case of the distal tibia, however, because stress concentrations in the distal extremity of the revision TKR prosthesis's extended stem with tibial baseplate can trigger excessive stress/strain in the distal tibia, which may cause pain,⁴⁹⁾ transferring high stress/strain to the distal tibia is considered rather undesirable.

Finally, the strain level of the tibia that can directly affect bone remodeling was verified to lie below the critical damage strain.⁵⁰⁾ These results demonstrate that the proposed revision TKR prosthesis has lower load shielding effects and lower risk of bone loss and negative bone reconstruction caused by excessive stress/strain effects compared to the control, which allows the assumption that its biomechanical stability is ensured.

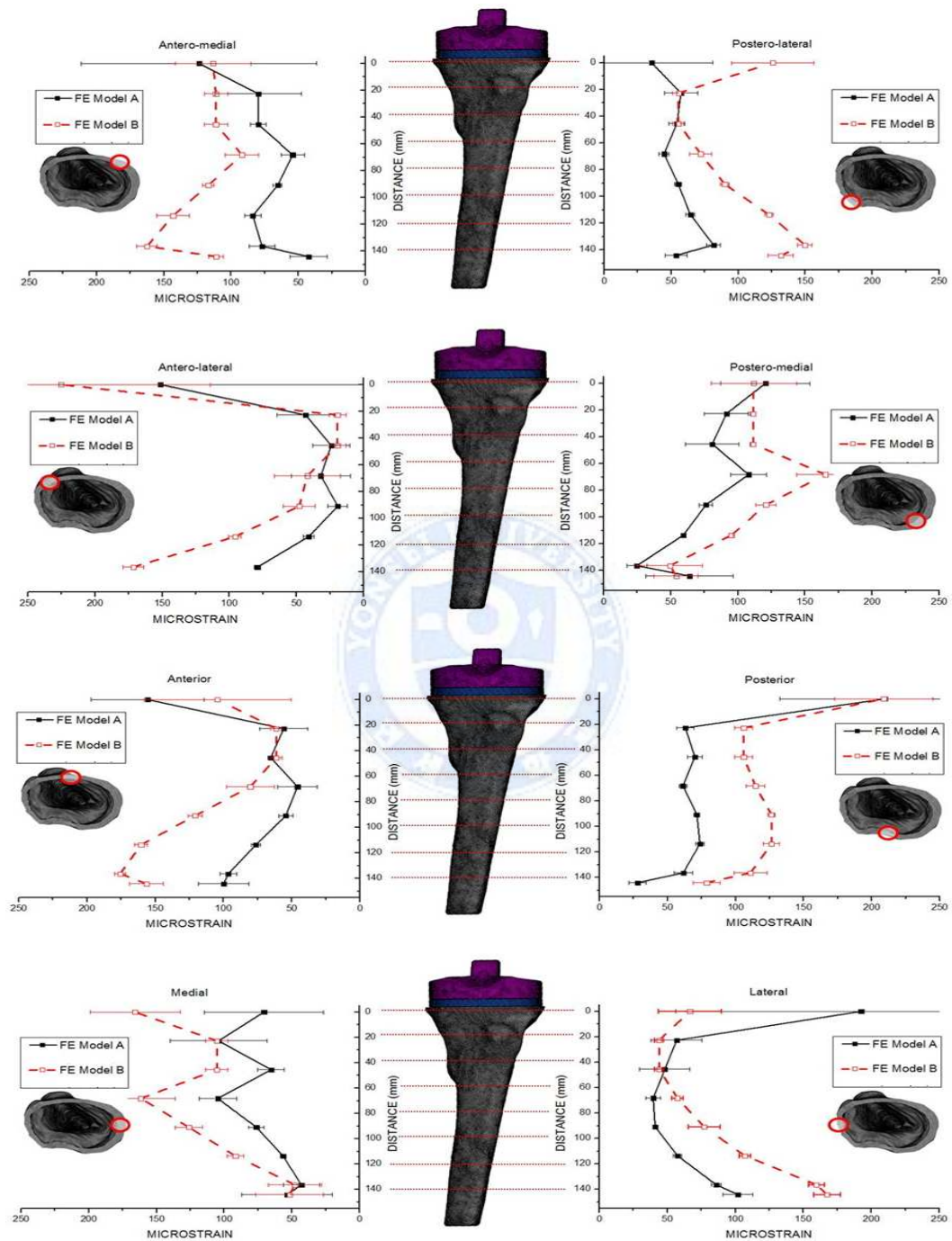


Fig. 40. The strain distribution in the tibia cortical bone(Model A : new R-TKR, Model B - commercial R-TKR)

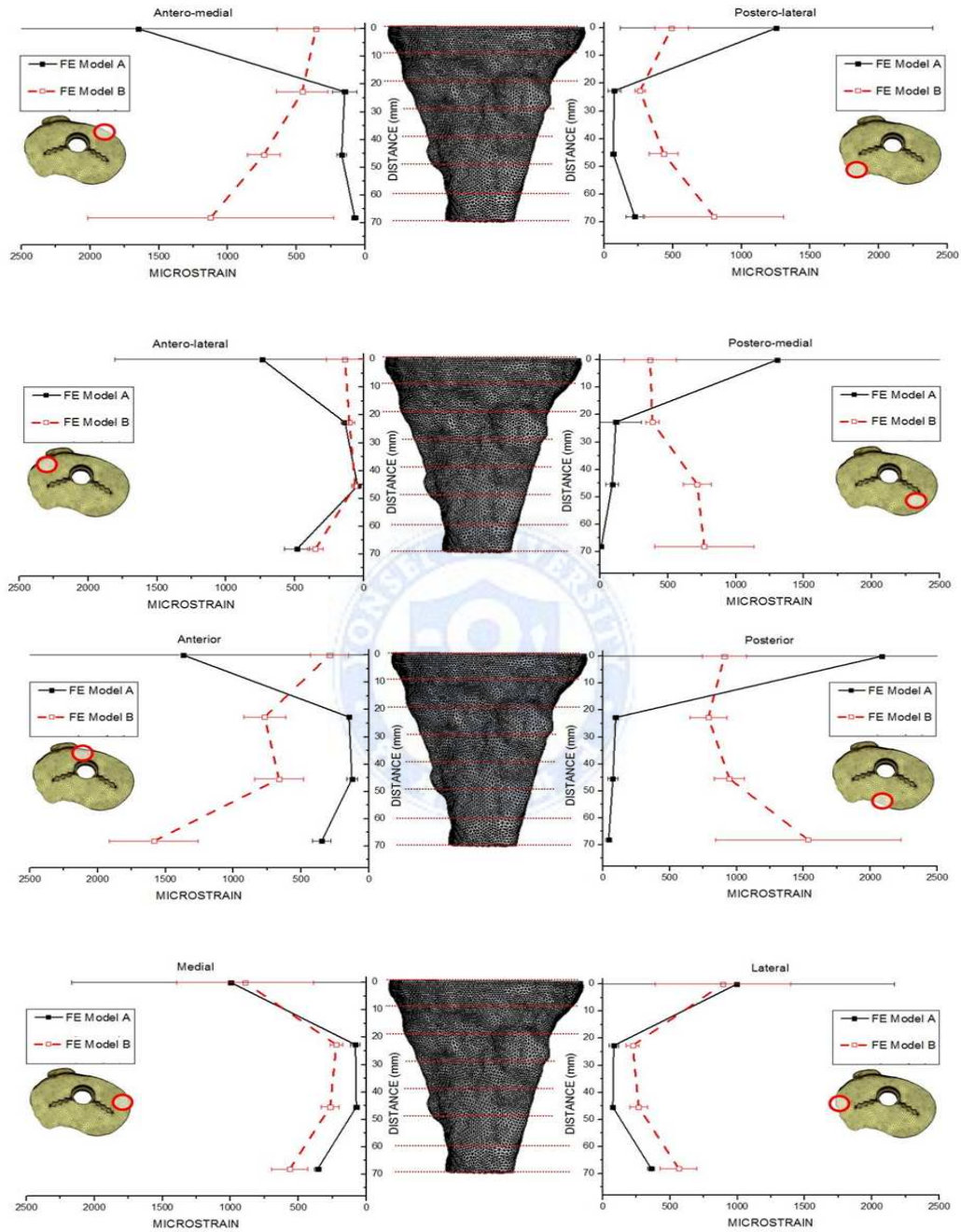


Fig. 41. The strain distribution in the tibia cancellous bone(Model A : new R-TKR, Model B - commercial R-TKR)

CHAPTER VI. BIOLOGICAL SAFETY EVALUATION

An artificial knee joint is a medical device that is inserted into the human body for a long period of time. As such, it is essential that sufficient biological safety should be provided for the raw materials and components as well as for the end products. As raw materials for artificial knee joints to be inserted into the knee joint, cobalt-chrome (CoCr) and titanium (Ti) are used for the femoral and tibial components, respectively, and for the insert, which functions as cartilage between the femoral and tibial components of the knee replacement, ultra-high molecular weight polyethylene is used. All of these materials possess high biocompatibility, and they are used in Korea as materials whose biocompatibility has been validated in compliance with international standards. A stem plug, a part that is additionally provided for revision TKR, is assembled to the threaded hole created around the stem housing of the femoral component and the tibial stem of the tibial baseplate for the purpose of preventing foreign bodies and hard/soft tissues from infiltrating into the threaded hole.



Fig. 42. The image of the stem plug

Currently, metal-based stem plugs are offered together with baseplates. In order to enhance industrial efficacy and reduce costs, a new material (Renshape - SL7870, HUNTSMAN) was developed as a replacement for metallic material for stem plugs. It was intended in this study that validation of the biological stability of the Renshape-based and 3D printing-generated stem plug inserted into the human body would be performed, thus testing its applicability.

In this study, for the biological safety validation in accordance with the national and international standard safety assessment methods, a cytotoxicity test, subcutaneous (intradermal) reactivity test, sensitization test, acute systemic toxicity test, and genotoxicity test (bacterial reverse mutation test – Ames test) were performed.

1. Cytotoxicity Test

This test was conducted on the test article to determine the potential for cytotoxicity in compliance with the procedures specified in the International Organization for Standardization, Biological Evaluation of Medical Devices – Part 5: Tests for In Vitro Cytotoxicity, ISO 10993-5, as well as the Common Standards Regarding the Biological Safety of Medical Devices of the Korea Food & Drug Administration(KFDA) – Tests for Cytotoxicity: in vitro Methods guidelines.

1.1 Cytotoxicity test method

The test article was tested in a minimum essential medium (MEM) with a ratio of 4.0 g/20 mL at 50°C for 72 h, and positive (zinc demethyldithiocarbamate [ZDEC] polyurethane film) and negative controls (high-density polyethylene [HDPE] film)

were extracted in the MEM with a ratio of 6 cm²/mL at 50°C for 72 h. The biological reactivity of a mammalian monolayer, L-929 mouse fibroblast cell culture, in response to the test article extract was determined. L-929 cells were grown in MEM, supplemented with 10% fetal bovine serum (FBS) and 1% antibiotic-antimycotic solution at 37°C in a 5% CO₂-humidified incubator. The test article or control article extracts were diluted 2-fold serially by adding fresh culture media (2 × MEM) containing 10% FBS and then used to replace the maintenance medium of the cell culture. All cultures were incubated for 24 h, under the same growth conditions as described above. After incubation, each culture was stained with MTT (3-(4,5-dimethylthiazol-2-yl)-2,5-diphenyl tetrazolium bromide) solution and lysed with DMSO (dimethyl sulfoxide) solution. Absorbance was measured at 570 nm with an automatic microplate reader. The relative cell viability was expressed as a percentage of the optical densities in the medium containing diluted extracts to the optical densities in the fresh control medium.

Table 10. Evaluation criteria of the cytotoxicity test

Grade	Reactivity	Observations	
0	None	Discrete intracytoplasmic granules	No lysis
1	Slight	Not more than 20% of the cells are round, loosely attached, and without intracytoplasmic granules	Not more than 20% lysis
2	Mild	Not more than 50% of the cells are round and devoid of intracytoplasmic granules	Not more than 50% lysis
3	Moderate	Not more than 50% of the cell monolayer contains rounded cells	Not more than 70% lysis
4	Severe	Nearly complete destruction of the cell monolayer	Greater than 70% lysis

1.2 Cytotoxicity test result

In the cytotoxicity test performed under the above-described conditions, a cell viability of 99% was observed in the extract of the test article SL7870, unlike the control. Cell vitality in excess of 95% was also observed when checked against the negative control. With the , the test article was determined to have zero cytotoxicity.

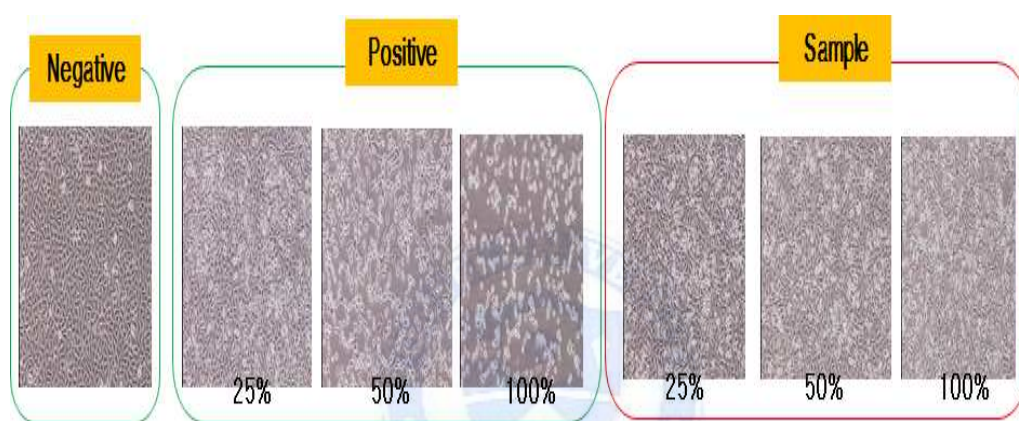


Fig. 43. The results of the cytotoxicity test

Table. 11. The results of the cell viability and reactivity grade in the cytotoxicity test

	Test article			Positive control			Negative control		
Extract concentration (%)	100	50	25	100	50	25	100	50	25
Cell viability (%)	95 ± 1	98 ± 1	99 ± 0	10 ± 0	49 ± 8	95 ± 1	100 ± 0	100 ± 0	100 ± 0
Reactivity Grade	1	1	1	4	3	1	0	0	0

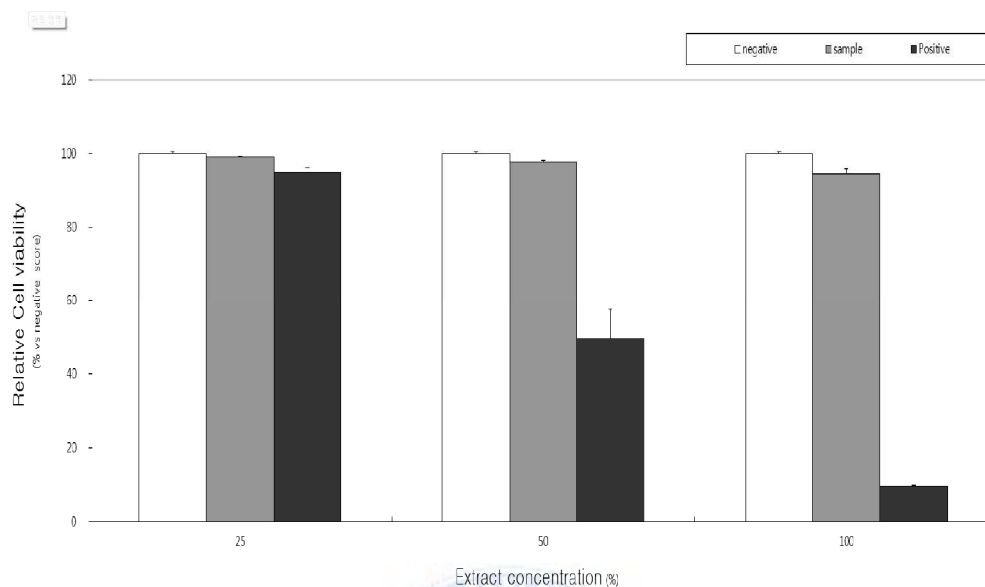


Fig. 44. Relative cell viability of the cytotoxicity test

2. Intracutaneous(intradermal) Reactivity Test

This study was conducted based on the procedures described in the International Organization for Standardization, Biological evaluation of medical devices - Part 10: Tests for irritation and skin sensitization, ISO 10993-10, and Common criteria in regard to biological evaluation of medical devices of the Korea Food & Drug Administration. This test was performed to determine whether chemicals that may leach or be extracted from the test article are capable of causing local irritation on rabbit dermal tissues.

2.1 Intracutaneous(intradermal) reactivity test method

A minimum of three healthy adult albino rabbits (New Zealand White variety) of either sex were obtained from an approved supplier, traceable in Yonsei

Medical Technology & Quality Evaluation Center records. All animals weighed in excess of the 2.0 kg minimum ISO weight limit. The test article was extracted in saline and CSO at a ratio of 4.0 g/20 mL at 50°C for 72 h. 0.2 mL of the extract obtained with polar or non-polar solvent was injected subcutaneously at five sites on one side of each rabbit. Similarly, 0.2 mL of the polar or non-polar solvent control was injected on five sites on the contralateral side of each rabbit. Observations for erythema and edema were carried out at 24, 48 and 72 h after the injections. The irritation reactions were scored on a 0 to 4 basis. Any adverse reactions at the test sites were also noted (Table 12).

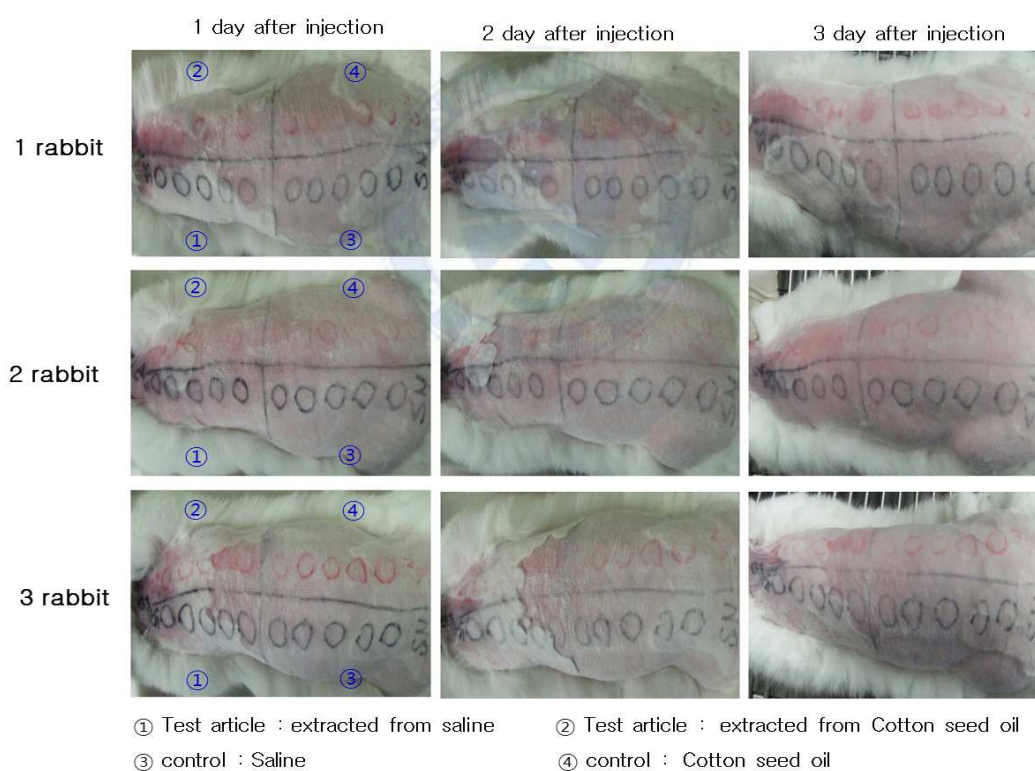


Fig. 45. The injection thermal site in intracutaneous(intradermal) reactivity test

Table 12. Dermal observation scoring in intracutaneous reactivity test

Erythema and eschar formation	Oedema formation
0 = No erythema	0 = No oedema
1 = Very slight erythema(barely perceptible)	1 = Very slight oedema (barely perceptible)
2 = Well-defined erythema	2 = Well-defined oedema (edges of area well-defined by definite raising)
3 = Moderate erythema	3 = Moderate oedema (raised ~1mm)
4 = Severe erythema (beet-redness) to eschar formation preventing grading of erythema	4 = Severe oedema (raised > 1mm and extending beyond exposure area)

2.2 Intracutaneous(intradermal) reactivity test result

The subcutaneous (intradermal) reactivity test performed in compliance with the test method specified in ISO 10993-10 Biological Evaluation of Medical Devices, Part 10: Tests for irritation and skin sensitization and the standards specified by the Ministry of Food and Drug Safety (MFDS) for the biological safety of medical devices yielded the following results: On visual inspection, the elute from the test article SL7870 did not trigger any skin reactions, such as erythema, crusting, and swelling, during the observation period after its application to the skin.(Table 13) Consequently, the average range of reactivity of the SL7870 elute was determined to be zero.

Table. 13. The results of intracutaneous reactivity test

Rabbit 1	24 h	48 h	72	Sum of Observation	Observation Average
Total Test(saline) Scores	0	0	0	0	0/15
Total Test(CSO) Scores	0	0	0	0	0/15
Total Control(saline) Scores	0	0	0	0	0/15
Total Control(CSO) Scores	0	0	0	0	0/15
Primary Irritation Score Test Observation Average (-) Control Observation Average					0
Rabbit 2	24 h	48 h	72	Sum of Observation	Observation Average
Total Test(saline) Scores	0	0	0	0	0/15
Total Test(CSO) Scores	0	0	0	0	0/15
Total Control(saline) Scores	0	0	0	0	0/15
Total Control(CSO) Scores	0	0	0	0	0/15
Primary Irritation Score Test Observation Average (-) Control Observation Average					0
Rabbit 3	24 h	48 h	72	Sum of Observation	Observation Average
Total Test(saline) Scores	0	0	0	0	0/15
Total Test(CSO) Scores	0	0	0	0	0/15
Total Control(saline) Scores	0	0	0	0	0/15
Total Control(CSO) Scores	0	0	0	0	0/15
Primary Irritation Score Test Observation Average (-) Control Observation Average					0

3. Irritation and Skin Sensitization Test

A guinea pig maximization test of the test article was conducted to evaluate the potential for delayed dermal contact sensitization. This study was conducted based on the procedures described in the International Organization for Standardization, Biological evaluation of medical devices - Part 10: Tests for irritation and skin sensitization, ISO 10993-10, and common criteria with regard to the biological evaluation of medical devices of the Korea Food & Drug Administration.

The test article was extracted in 0.9% sodium chloride (saline) and cottonseed oil (CSO) with a ratio of 4.0 g/20 mL at 50°C for 72 h. Each extract was intradermally injected into ten test guinea pigs (per extract) in an attempt to induce sensitization. The vehicles (negative control) were similarly injected into five control guinea pigs (per vehicle). Following a recovery period, the test and control animals received a challenge patch of the appropriate test article extract and reagent control. All sites were scored at approximately 24 and 48 hours after patch removal.

3.1 Irritation and skin sensitization test method

The guinea pig maximization test was performed to evaluate the potential for delayed dermal contact sensitization of the test article. A minimum of 35 healthy adult albino guinea pigs were obtained from an approved supplier, traceable in Yonsei Medical Technology & Quality Evaluation Center records. The range of animal weights at first treatment was 300 g to 500 g. Ten test guinea pigs (saline extract) and ten test guinea pigs (CSO extract) were injected with the test article and Freund's complete adjuvant (FCA). Five guinea pigs (negative control: saline), and five guinea pigs (negative control: CSO) were injected with the corresponding control blank and FCA (intradermal induction phase).

Table. 14. The preparation of irritation and skin sensitization test

Negative Control:	0.9% sodium chloride(saline) & Cotton oil(CSO)
Positive Control:	0.05% DNCB(2,4-Dinitrochlorobenzene)
Preparation:	The samples were prepared aseptically. The test article was extracted in saline and CSO with a ratio of 4.0g/20mL at 50°C for 72h.
Additional Materials:	Freund's Complete Adjuvant(FCA) was mixed 50:50(v/v) with the chosen vehicle and used at induction I. A 10% sodium dodecyl sulfate (SDS) suspension in petrolatum was used for induction II.
Test animals:	Healthy young adult albino guinea pigs : total 35 (Negative control – per vehicles : 5, Test group – per extract : 10, Positive control : 5)

On day 6, the areas on the injection sites were treated with 10% sodium dodecyl sulfate (SDS). On the day following SDS treatment, topical patches with the appropriate test extract were applied to the test animals, and topical patches with the corresponding control blank were applied to the control animals (topical induction phase). The patches were removed after 48 h of exposure. Following a 2-week rest period, topical patches were applied to the test animals on a previously untreated area with the appropriate test extract, while the same was done for the control animals using a control blank (challenge phase). The patches

were removed after 24 h of exposure. The dermal patch sites were observed for erythema and edema 24 and 48 h after patch removal. Each animal was assessed for a sensitization response based upon dermal scores (Table 15).

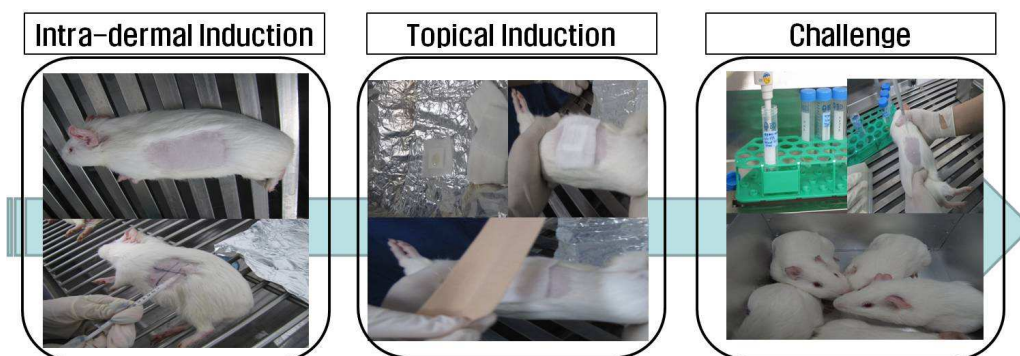


Fig. 46. The procedure of the irritation and skin sensitization test

Table. 15. Magnusson and Kligman scale

Patch test reaction	Grading scale
No visible change	0
Discrete or patchy erythema	1
Moderate and confluent erythema	2
Intense erythema and/or swelling	3

3.2 Irritation and skin sensitization test results

In the irritation and skin sensitization test on the extract of the test article SL7870, no skin sensitization was exhibited, nor was any difference noticeable when compared with the negative control.

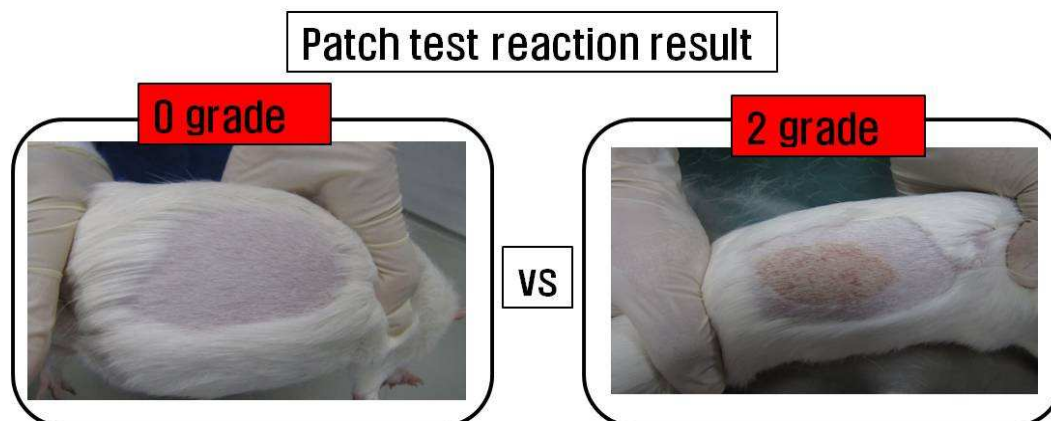


Fig. 47. The results of the Irritation and skin sensitization test

Table. 16. Negative control, test article extract, and positive control observation after challenge phase

group	observation	Mean score	Number of animal									
			1	2	3	4	5	6	7	8	9	10
Negative control (Saline)	24hr	0	0	0	0	0	0					
	48hr	0	0	0	0	0	0					
Test Article (Saline)	24hr	0	0	0	0	0	0	0	0	0	0	0
	48hr	0	0	0	0	0	0	0	0	0	0	0
Negative control (Cotton oil)	24hr	0	0	0	0	0	0					
	48hr	0	0	0	0	0	0					
Test Article (Cotton oil)	24hr	0	0	0	0	0	0	0	0	0	0	0
	48hr	0	0	0	0	0	0	0	0	0	0	0
*Positive control (0.05% DNCB)	24hr	2	2	2	2	2	2					
	48hr	2	2	2	2	2	2					

4. Acute Systemic Toxicity Test

This study was conducted based on the procedures described in the International Organization for Standardization, Biological evaluation of medical devices - Part 11: Tests for systemic toxicity, ISO 10993-11, and common criteria regarding biological evaluation of medical devices of the Korea Food & Drug Administration. The tests for acute systemic toxicity: in vivo methods guidelines were followed in tests conducted on the test article to determine the potential for acute systemic toxicity.

4.1 Acute systemic toxicity test method

At least five male animals (ICR mice) per test extract and per negative control vehicle were employed. The range of animal weights at first treatment was 17 g to 23 g. The test article was extracted in saline and CSO at a ratio of 4.0 g/20 mL at 50°C for 72 h. Each extract was intravenously or intraperitoneally injected to five test animals (per extract).

Table. 17. Acute systemic toxicity test materials

Negative Control(Vehicles):	0.9% sodium chloride(saline) & Cotton oil(CSO)
Preparation:	The samples were prepared aseptically. The test article was extracted in saline and CSO with a ratio of 4.0g/20mL at 50°C for 72h.
Test animals:	Healthy young adult ICR mice : total 20 (Negative control – per vehicles : 5, Test group – per extract : 5)
Dosage:	50mL/kg/head

Each vehicle (negative controls) was similarly injected into five control animals (per vehicle) (Table 18). The animals were observed immediately after injection, and then 4, 24, 48, and 72 hours after injection. All animals were weighed prior to injection and after the final observation.

Table 18. Acute systemic toxicity test condition

Group		Dose per kg	Route*	Injection Rate µl per second
Negative control (Vehicles)	0.9% Sodium Chloride	50mL	IV	100
	Cotton oil	50mL	IP	100
Test article (Extract)	0.9% Sodium Chloride	50mL	IV	100
	Cotton oil	50mL	IP	100

*IV = Intravenous, IP = intraperitoneal

4.2 Acute systemic toxicity test results

This test was conducted on the test article in compliance with the procedures specified in the ISO 10993-11 Biological Evaluation of Medical Devices, Part 11: Tests for systemic toxicity as well as the Common Standards Regarding the Biological Safety of Medical Devices provided by the MFDS. All animals survived the observation period after the injection of the extracts of the test article SL7870(Fig. 48) and no abnormal changes were observed in skin, hide, eyes, respiratory system, circulatory system, nerve system, behavioral patterns, and body weight.(Fig. 49) Thus, it was verified that the extract of SL7870 did not show acute systemic toxicity.



Fig. 48. Acute systemic toxicity test result : no mice with death, abnormality and body weight loss.

Table 19. Acute systemic toxicity test result

Time	Negative Control		Test Article	
	0.9% Sodium Chloride	Cotton oil	0.9% Sodium Chloride	Cotton oil
4hours after Injection	P	P	P	P
24hours after Injection	P	P	P	P
48hours after Injection	P	P	P	P
72hours after Injection	P	P	P	P

P (Pass): If a body weight loss of greater than tow g does not occur in three or more mice, the test article meets the requirements of the test.

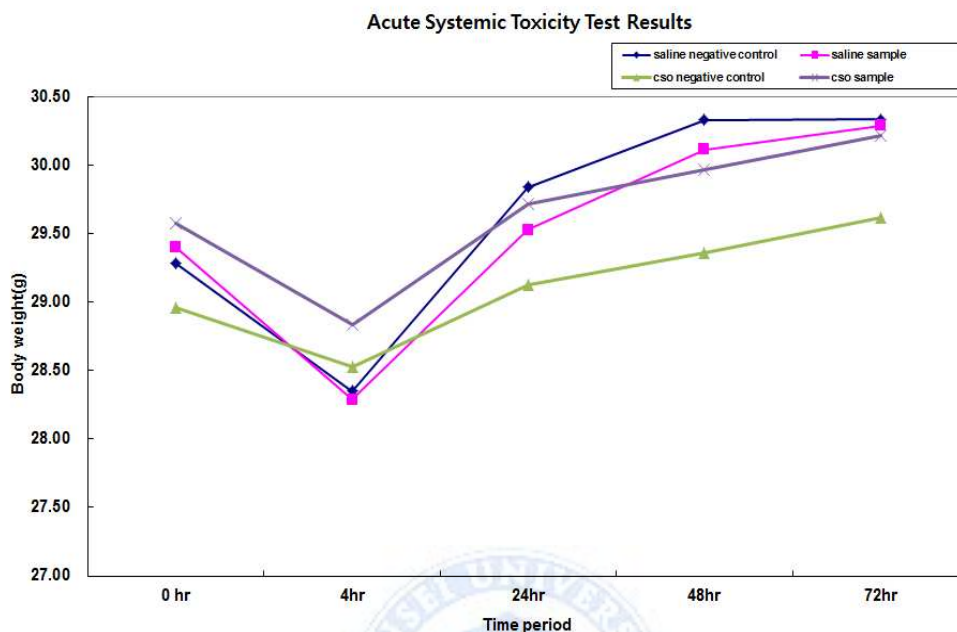


Fig. 49. The body weight changes on Acute systemic toxicity test

5. Genotoxicity test (bacterial reverse mutation test-Ames test)

This *Salmonella typhimurium*-reverse mutation standard plate incorporation study was conducted to evaluate whether a 0.9% sodium chloride (saline) / dimethyl sulfoxide (DMSO) extract of the test article would cause mutagenic changes in the average number or revertants for histidine-dependent *S. typhimurium* strains TA97, TA98, TA100, and TA1535, and *Escherichia coli* WP2uvrA in the presence and absence of S9 metabolic activation. This study was conducted based on the procedures described in the OECD Guideline for the Testing of Chemicals 471, Bacterial Reverse Mutation Test and common criteria regarding biological evaluation of medical devices of the Korea Food & Drug Administration.

5.1 Genotoxicity test (bacterial reverse mutation test - Ames test) method

The test article was extracted in saline and DMSO at a ratio of 4.0 g/20 mL at 50°C for 72 h. The extract was found to be non-inhibitory to growth of the tester strains.

Table. 20. Bacterial Reverse Mutation Test - Ames test materials

Vehicles:	0.9% sodium chloride (Saline) 4% dimethyl sulfoxide (DMSO)
Preparation:	The samples were prepared aseptically. The test article was extracted in saline/DMSO with a ratio of 4.0g/20mL at 50°C for 72h. Vehicle without test material was similarly subjected to the extraction conditions for use as a negative control. The test extract and negative control were decanted.
Target strain:	Salmonella typhimurium : TA97, TA98, TA100, TA1535 Escherichia coli : WP2uvrA
Positive control (Mutagens): with S9 mix	For Test Strain TA97, 2-aminoanthracene(2-AA) For Test Strain TA98, 2-aminoanthracene(2-AA) For Test Strain TA100, 2-aminoanthracene(2-AA) For Test Strain TA1535, 2-aminoanthracene(2-AA) For <i>Escherichia coli</i> WP2uvrA, methyl methanesulfonate (MMS)
Positive control (Mutagens): without S9 mix	For Test Strain TA97, ICR-191 For Test Strain TA98, 4-nitroquinoline N-oxide(NQNO) For Test Strain TA100, methyl methanesulfonate (MMS) For Test Strain TA1535, Sodium azide (SA) For <i>Escherichia coli</i> WP2uvrA, methyl methanesulfonate (MMS)
Media:	Minimal glucose agar medium : 1X Vogel-Bonner salt solution + 2% glucose+ 1.5% agar

Mammalian metabolic activation systems (S-9 activation mix, composed mainly of the microsomal fraction from an Aroclor 1254-induced rat liver homogenate), which contain enzymes that perform several metabolic conversions similar to those of mammalian organs, were used in the test system for the detection of mutagenic chemicals. Aliquots of the test extract and both positive and negative control solutions were added to triplicate plates containing histidine-deficient medium with and without the S-9 mix. Separate plates were inoculated with the Ames *S. typhimurium* tester strains TA97, TA98, TA100, and TA1535, and *E. coli* WP2uvrA. Briefly, separate tubes containing 2 mL of molten top agar supplemented with histidine-biotin solution of the *S. typhimurium* strain was inoculated with 0.1 mL of culture for each five tester strains, and 0.1 mL of the saline/DMSO extract. The test extract and both positive and negative control solutions were added to triplicate plates containing histidine-deficient medium with and without the S-9 mix. All plates in a given assay were incubated at 37°C for 48-72 hours. After the incubation period, the number of revertant colonies per plate was counted. The rate of mutation to non-histidine-dependent wild types was determined for each plate: the spontaneous reversion rate for each strain in the presence of the saline blank was compared to the corresponding rate of reversion in the presence of the test article extract and in the presence of known mutagens.

Table 21. S-9 mixture condition

S-9 mix (Rat liver enzyme + microsomal cofactors)	8 mM MgCl ₂ +33mMKCl
	5 mM Glucose-6-phosphate
	4 mM NADP
	100 mM Sodium phosphate buffer(pH7.4)
	Rat liver S9 (0.04mL / mL of mix)

5.2 Genotoxicity test (bacterial reverse mutation test - Ames test) results

The test results were displayed as the average value of the counts of three plates per test strain. The result was considered positive when the number of revertant colonies of at least one strain consistently increased compared to the controls and when the test was positive in at least one strain, regardless of the use of metabolic activation systems, or when a reproducible increase was shown.

The extract of the test article SL7870 exhibited similar counts of revertant colonies in all test strains when compared with the negative control solutions.

The counts of revertant colonies of all positive control solutions substantially increased compared to the negative control solutions, thus proving that the test was performed correctly.

Table. 22. Ames plate incorporation assay For 0.9% sodium chloride(saline) extract

Salmonella typhimurium Tester Strains	Number of Revertant Colonies (Average of triplicate plates)		
	Negative Control	Test Article Extract	Positive Control *
TA97 without S-9	345	304	>5000
TA98 without S-9	265	255	1597
TA100 without S-9	273	252	1637
TA1535 without S-9	23	23	979
Escherichia coli WP2uvrA	82	95	1559
TA97 with S-9	296	239	1824
TA98 with S-9	268	296	1936
TA100 with S-9	301	269	2172
TA1535 with S-9	18	22	647
Escherichia coli WP2uvrA	146	203	2781

Table. 23. Ames plate incorporation assay For 4% dimethyl sulfoxide (DMSO) extract

Salmonella typhimurium Tester Strains	Number of Revertant Colonies (Average of triplicate plates)		
	Negative Control	Test Article Extract	Positive Control *
TA97 without S-9	287	340	>5000
TA98 without S-9	236	277	1597
TA100 without S-9	299	249	1637
TA1535 without S-9	30	27	979
Escherichia coli WP2uvrA	109	105	1559
TA97 with S-9	223	302	1824
TA98 with S-9	250	290	1936
TA100 with S-9	287	265	2172
TA1535 with S-9	22	25	647
Escherichia coli WP2uvrA	185	175	2781

* without S-9: TA 97 = ICR 191, TA 98 = 4-nitroquinoline-N-oxide, TA 100 = methyl-methanesulfonate, TA 1535 = sodium azide, Escherichia coli WP2uvrA = methyl-methanesulfonate

* with S-9: TA 97 = 2-aminofluorene (2-AF), TA 98, TA 100, TA 1535 = 2-aminoanthracene (2-AA), Escherichia coli WP2uvrA = methyl-methanesulfonate

CHAPTER V. CONCLUSIONS AND FUTURE WORK

The knee joint is constantly subjected to repeated weight-bearing loads and is prone to injury or functional decline. In severe cases, such as degenerative arthritis, where conservative therapies show little improvement, total knee arthroplasty (TKA) has proven to be an efficient treatment option with good clinical outcomes.¹⁾²⁾⁷⁾¹³⁾ Patients requiring TKA need to undergo primary TKA as the initial replacement surgery and revision TKA as the follow-up surgery after the end of the service life of the primary total knee replacement (TKR) prosthesis.

Because of the repetitive and constant nature of knee joint motions, wear of the tibial spacer articular surface, loosening of prosthetic components, instability, and fracture are known as major causes for revision TKA.¹³⁾²⁶⁾ According to the reports of Carr et al. the number of patients that undergo revision TKA due to the failure of primary TKA increased by 3–6% every year between 2001 and 2009.¹⁴⁾

In an effort to improve the service life of knee replacements, extensive studies have been conducted.¹⁷⁾²¹⁾ A variety of studies have investigated design for wear mitigation, improved baseplate design for enhancing stress transfer, and keel design.³¹⁾ Many studies have focused on enhancing durability and structural stability, such as with surface or material improvements to enhance the post-insertion stability. As a result, a wide range of products have been commercialized. In Korea, the supply of revision TKR prostheses depends on imports from global companies, and revision TKR prostheses require domestic research and development.

This study was conducted to analyze the clinical and mechanical design

elements of revision total knee replacement systems based on the primary artificial knee joints currently in use and to develop a new revision TKR prosthesis by performing various tests and evaluations. To achieve this goal, clinical requirements were analyzed and a system that satisfied those requirements was implemented. The newly developed revision TKR prosthesis was then subjected to various mechanical function and biological stability tests to validate its clinical applicability and establish a research frame for producing domestic revision TKR prostheses.

To implement the design of a new revision TKR prosthesis, three design elements, namely stability, modularity, and safety, were taken into account in analyzing the detailed design elements and product design. The ranges of motion (ROMs) for the new revision TKR prosthesis were configured to have limited levels in consideration of the limited movement abilities and activity levels of the users, on the one hand, and the increased need for stability on the other. In other words, it was intended to enhance stability by enhancing conformity. Additionally, anatomical shapes were taken into consideration to strengthen the support frame of the revision TKR prosthesis, and the femur stem extension, tibial baseplate, and stem extension were designed accordingly. Furthermore, reconstruction parts were introduced in order to compensate for bone resection and to restore bone loss, and the tibial insert post was designed to be concave-shaped to increase safety by preventing dislocation through increased jump distance.

The performance features of the proposed revision TKR were evaluated with a variety of tests. Structural stability is a key factor by the inherent nature of the knee joint. Structural stability and the stability of each connector were validated using the finite element analysis (FEA) method. As a result, it was verified that

structural stability was provided in all parts except for the tibial baseplate. As for the tibial baseplate, however, since its structural strength decline of 23% was caused by the hole design to assemble the reconstruction parts, which is a distinctive feature of the revision TKR prosthesis, sufficient structural stability may be provided once inserted into the body, considering the yield stress of CoCr and high load level. Additionally, although high stress was generated in the bond strength test due to the insertion angle, no safety problem is expected to arise in the connector in relation to load conditions.

As additional revision TKR stability tests, fatigue tests and assembly locking tests were conducted. Fatigue load was applied to the proposed TKR prosthesis in accordance with the ASTM test method to investigate the failure feature. No fracture or crack was observed, even under the application of a load higher than the ASTM guideline standard. The bond strength between the stem extension and offset adapter was tested by the assembly and disassembly torque test. The result indicated an assembly-to-disassembly torque ratio ranging between 99.7% and 101% (average: 100.5%), thus demonstrating that stability was sufficiently reflected in the proposed revision TKR prosthesis.

Besides the evaluation of its structural and mechanical stability, the evaluation of the effects of load transfer of the revision TKR prosthesis on the tibia is an important factor. It is well known that the stress concentration and stress shielding induced by knee replacement during insertion can cause fracture, pain, and loosening induced by bone resorption. Thus, load distribution in the tibia is an important factor from the biomechanical point of view. Therefore, a finite element model (FEM) of the tibial component of the proposed revision TKR prosthesis was created for the evaluation of structural stability as well as the stress/strain

distribution behavior in the tibia after the insertion.

A FEM-based implant model, in which the proposed revision TKR was inserted, was implemented for testing and evaluation purposes. Stability was tested by comparing the yielding stress, taking into account the safety factor, and the peaked von Mises stress (PVMS) of the tibial and femoral components. The resulting values were less than 10% in the tibial component of the proposed revision TKR prosthesis and less than 70% in the tibial cortical and cancellous bones each, suggesting that the proposed TKR prosthesis does not need any additional improvement or supplement in design elements for application. As such, structural stability is sufficiently provided under the aspect of tibial fracture risk.

The impact of the tibial component of the proposed revision TKR prosthesis on the host tibia was evaluated by analyzing the stress/strain distributions between the proximal and distal extremities of the tibia. Additionally, a real-life revision TKR model was implemented for comparative analysis. Relatively high stress/strain levels were observed at the cortical and cancellous bonds, and the stress/strain levels of the cancellous bone increased as the load moved towards the distal part. This is assumed to be caused by the keel design and stem insertion angle designed to prevent rotation. This implies that adequate stress/strain can be generated in the cortical and cancellous bones during the insertion of the proposed revision TKR, which is expected to mitigate the loosening-related problem due to stress-shielding effects and increase in bond resorption. Furthermore, the estimated strain was verified to lie below the critical damage strain that can directly affect bone remodeling, as reported by Pattin et al. Finally, the proposed revision TKR prosthesis was compared with an existing product with a high market share. As a result, it was verified that generally similar stress/strain distribution patterns were

shown when the tibial component of the revision TKR prosthesis was inserted. Moreover, a higher average strain was shown in the proximal part and a lower average strain was shown in the distal part. These results suggest that the tibial component of the proposed revision TKR prosthesis showed slightly improved stress-shielding effects in the proximal tibia, and the proposed revision TKR prosthesis is expected to have an improved biomechanical performance compared to the revision TKR prosthesis with a high international market share.

Since an artificial knee joint is a medical device that is inserted into the human body for a long period of time, its biological safety should be ensured. For the development of a new revision TKR prosthesis, the hole plug, for which metal is usually used, was fabricated with a new material, SL7870, using the 3D printing method, and its biological safety was validated in the cytotoxicity, subcutaneous (intradermal) reactivity, sensitization, acute systemic toxicity, and genotoxicity tests. The cytotoxicity test revealed that the extract of the test material was non-toxic by verifying 99% cell viability. In the subcutaneous (intradermal) reactivity test using rabbits, the extract of the test material did not trigger skin reactions such as erythema, crusting, and swelling. Nor did the sensitization test reveal any abnormal reactions on the skin of the mice exposed to stimuli. The acute systemic toxicity test did not trigger any abnormal changes in skin, hide, eyes, and body weight. Finally, in the genotoxicity test, no significant differences were observed in the results of mutagenicity of microorganisms between the test material and negative controls. The biological safety of the new material was thus proved.

In this study, the clinical and anatomical requirements for revision TKR prostheses were analyzed for the purpose of developing a new revision TKR prosthesis. Detailed parameters for important factors were analyzed, and a design

meeting all the requirements was implemented. A variety of validation and testing methods were established in order to evaluate whether the designed product meets the functional and biomechanical requirements under the structural, mechanical, and biological aspects. The analysis results of various tests performed on the newly developed revision TKR prosthesis verified its applicability and marketability. In this study, stability evaluation was performed from various viewpoints so that the design reflecting the clinical requirements and evaluation methodologies related to safety validation could be explored. This study is significant in that it first provided the basic data for the development of a domestically produced revision TKR prosthesis. Based on the results of this study, research will be continued with the intent to obtain approval for the proposed revision TKR prosthesis through its efficacy validation and clinical trials. The achievement of this study is expected to contribute to the research and development of domestically produced revision TKR prostheses for the domestic market, which is currently dominated by imported products.

REFERENCE

1. Giles. R. Scuderi, Alfred J Tria, Jr. "The knee, A Comprehensive Review" 2010
2. "The Knee 2013", Korean knee society, 2013
3. Google image, "ligament location tibia", <http://z0mbie.host.sk/Tibial-Plateau-Fractures.html>, 2014. 12
4. Google image, "patellar", <http://www.chiropractic-help.com/Patello-Femoral-Pain-Syndrome.html>, 2014.12
5. Google image, "muscle knee", <http://healthfavo.com/knee-joint-muscles.html/knee-joint-muscles-2>, 2014.12
6. Google image, "ligament knee", <http://www.humankinetics.com/excerpts/excerpts/many-ligaments-make-up-knees-structure>, 2014.12
7. Google image, "motion of knee", <http://www.militarydisabilitymadeeasy.com/kneeandleg.html>, 2015.01
8. Susan J Hall, Ph.D "Basic Biomechanics second edition" 1995
9. Margareta nordin, "Basic Biomechanics of the Musculoskeletal system, 3th", 2003
10. Reilly DT, Martens M, "Experimental analysis of the quadriceps muscle force and patellofemoral joint reaction forces for various activities." Acta Orthop Scand, vol. 43, pp.126-137, 1972
11. Della Valle C, Rosenberg A, "Indications for total knee arthroplasty. In: Callahan J, ed. The adult knee. 1st ed. Philadelphia: Lippincott williams & Wilkins" pp.1047-1058, 2003
12. A. J. Bailey, C. Buckland-Wright, D. Metz, "The role of bone in osteoarthritis" Age Ageing, vol. 30, no. 5, pp.374-378, 2001
13. E. Rubin, JL. Farber, "Bone and Joints: Pathology 2nd edition", pp. 1273-2347, 1994
14. A. J. Carr, O. Robertsson, S. Graves, "Knee replacement" Lancet, vol. 379, no. 9823, pp.1331-1340, 2012
15. Kurtz S, Ong K, Lau E, Mowat F, Halpern M, "Projection of primary and revision hip and knee arthroplasty in the united states from 2005 to 2030" J Bone Joint Surg Am vol. 89 no. 4 pp.780-785, 2007
16. Freeman MA, Pinskerova V "The movement of the knee studied by

- functional analysis based on postmortem studies: J Bone Joint Surg, vol. 58-A, pp.179-185, 1976
17. I. H. Yang "Review Article : History of Total Knee Replacement" Knee surgery & Related Research, vol. 22, no. 2, 2010
 18. C. J. Lavernia, M. K. Drakeford, and A. K. Tsao, "Revision and primary hip and knee arthroplasty. A cost analysis," Clin Orthop Relat Res, vol. no. 311, pp.136-141, 1995
 19. K. P. Emmerson, C. G. Moran, and I. M. Pinder, "Survivorship analysis of the Kinematic Stabilizer total knee replacement: a 10- to 14-year follow-up," J Bone Joint Surg Br, vol. 78, no. 3, pp.441-445, 1996
 20. C. S. Ranawat, C. P. Luessenhop, and J. A. Rodriguez, "The press-fit condylar modular total knee system. Four-to-six-year results with a posterior-cruciate-substituting design," J Bone Joint Surg Am, vol. 79, no. 3, pp.342-348, 1997
 21. Tsonga, S. Kapetanakis, C. Papadopoulos, J. Papathanasiou, N. Mourgias, N. Georgiou, A. Fiska, K. Kazakos "Evaluation of Improvement in Quality of Life and Physical Activity After Total Knee Arthroplasty in Greek Elderly Women" The Open Orthopaedics Journal, vol. 5, pp.343-347, 2011
 22. J. Weir, C.G. Moran, I. M. Pinder "Kinematic condylar total knee arthroplasty 14-year survivorship analysis of 208 consecutive." J Bone Joint Surg[Br] vol.78-B, no. 6, 1996
 23. Dev S. Gill, Atul B. Joshi, "Long-term results of Kinematic Condylar knee replacement" J Bone Joint Surg vol.83, no. 3, pp.355-358, 2001
 24. Ducheyne, A. Kagan, 2nd and J. A. Lacey, "Failure of total knee arthroplasty due to loosening and deformation of the tibial component." J Bone Joint Surg Am, vol. 60, no. 3, pp.384-391, 1978
 25. N. Insall, R. W. Hood, and L. B. Flawn, "The total condylar knee prosthesis in gonarthrosis. A five to nine-year follow-up of the first one hundred consecutive replacements." J Bone Joint Surg Am, vol. 65, no. 5, pp.619-628, 1983
 26. Sharkey PF, Hozack WJ, Rothman RH, Shast "Insall Award paper, Why are total knee arthroplasties fail today" clin Orthop Relat Res, vol. 404 pp.7-13, 2002
 27. Peter F. Sharkey, MD, Paul M. Lichstein, MD, MS, Chao Shen, MD, Anthony T. Tokarski, BS, Javad Parvizi, MD, FRCS "Why are total knee

- arthroplasties failing today-has anything changed after 10 years" J. arthro. vol. 29 pp.1774-1778, 2014
28. Matthew S. Austin, MD, Peter F. Sharkey, MD, William J. Hozack, MD, Richard H. Rothman, MD, PhD "Knee failure mechanisms after total knee arthroplasty" Techniques in knee surgery, vol. 3, no. 1 pp.55-59, 2004
 29. G. H. Van Lenthe, M. C. de Waal Malefijt, and R. Huiskes, "Stress shielding after total knee replacement may cause bone resorption in the distal femur," J Bone Joint Surg Br, vol. 79, no. 1, pp.117-122, 1997
 30. D. Taylor, "Bone maintenance and remodeling: a control system based on fatigue damage," J Orthop Res, vol. 15, no. 4, pp.601-606, 1997
 31. J. W. Barrington, A. Sah, and H. Malchau, "Contemporary Cruciate-retaining total knee arthroplasty with a pegged tibial baseplate. Results at a minimum of ten years," J bone Joint Surg Am, vol. 91 no. 4, pp.874-878, 2009
 32. Steven L. Barnett, Ryan R. Mayer, Joseph S. et al, "Use of Stepped Porous Titanium Metaphyseal Sleeves for Tibial Defects in Revision Total Knee Arthroplasty : Short Term Results" J. Arthro. vol. 29, pp.1219-1224, 2014
 33. "Medical device market research reports - Artificial knee joint", KHIDI, 2013,
 34. "The medical device production, export, import reports in korea" MDFS, 2013
 35. T. K. Fehring, S. Odum, and C. Olekson, "Stem fixation in revision total knee arthroplasty: a comparative analysis," Clin Orthop Relat Res, vol. no. 416, pp.217-224, 2003
 36. A. Completo, J.A. Simoes, F. Fonseca "Revision total knee arthroplasty : the influence of femoral stems in load sharing and stability" The Knee, vol 16, pp.275-279, 2009
 37. ASTM F1223-08, Standard Test Method for Determination of Total Knee Replacement Constraint
 38. ASTM F1800-12. Standard Test Method for Cyclic Fatigue Testing of Metal Tibial Tray Components of Total Knee Joint Replacements
 39. ASTM F1814-97a(2009) Standard Guide for Evaluating Modular Hip and Knee Joint Components
 40. H. D. Clarke, R. T. Trousdale, "Component fracture in total knee arthroplasty," Knee, vol. 6, no. 4, pp.261-267, 1999

41. M. Taylor, K. E. Tanner and M. A. Freeman, "Finite element analysis of the implanted proximal tibia: a relationship between the initial cancellous bone stresses and implant migration," J Biomech, vol. 31, no. 4, pp.303-310, 1998
42. U. Simon, P. Augat, A. Ignatius, "Influence of the stiffness of bone defect implants on the mechanical conditions at the interface: a finite element analysis with contact," J Biomech, vol. 36, no. 8, pp.1079-1086, 2003
43. A. G. Au, A. B. Liggins, V. J. Raso, "A parametric analysis of fixation post shape in tibial knee prostheses," Med Eng Phys, vol. 27, no. 2, pp.123-134, 2005
44. A. G. Au, V. James Raso, A. B. Liggins, "Contribution of loading conditions and material properties to stress shielding near the tibial component of total knee replacements," J Biomech, vol. 40, no. 6, pp.1410-1416, 2007
45. N. A. Ramaniraka, L. R. Rakotomanana and P. F. Leyvraz, "The fixation of the cemented femoral component. Effects of stem stiffness, cement thickness and roughness of the cement-bone surface," J Bone Joint Surg Br, vol. 82, no. 2, pp.297-303, 2000
46. M. Tew, W. Waugh, "Tibiofemoral alignment and the results of knee replacement," J Bone Joint Surg Br, vol. 67, no. 4, pp.551-556, 1985
47. I. J. Harrington, "A bioengineering analysis of force actions at the knee in normal and pathological gait," Biomed Eng, vol. 11, no. 5, pp.167-172, 1976
48. A. Completo, A. Rego, and F. Fonseca, "Biomechanical evaluation of proximal tibia behaviour with the use of femoral stems in revision TKA: an in vitro and finite element analysis," Clin Biomech (Bristol, Avon), vol. 25, no. 2, pp.159-165, 2010
49. R. L. Barrack, C. Rorabeck, and M. Burt, "Pain at the end of the stem after revision total knee arthroplasty," Clin Orthop Relat Res, vol. no. 367, pp.216-225, 1999
50. C. A. Pattin, W. E. Caler, and D. R. Carter, "Cyclic mechanical property degradation during fatigue loading of cortical bone," J Biomech, vol. 29, no. 1, pp.69-79, 1996

국 문 요 약

생체역학적 안정성 및 생물학적 안전성 평가를 통한 재치환용 인공무릎관절의 개발 연구

권 순 영

생체공학협동과정

연세대학교 대학원

인체의 가장 큰 관절 중 하나인 무릎관절은 넓은 운동범위(range of motion)와 함께 반복적인 하중 및 지속적인 운동에 노출되어 있어, 관절의 손상 위험성이 타 관절에 비해 상대적으로 높다. 최근 고령화 및 사회 활동 참여 확대로 관절 퇴행 등 관절 질환이 증가하고 있고, 이는 무릎관절의 운동 기능 제한과 통증을 유발하고 나아가 삶의 질을 저해하는 원인으로 지적되고 있다.

무릎관절의 통증완화 및 운동기능 회복을 위해 보전적 치료법부터 수술적 치료법등 다양한 치료술이 존재하지만, 퇴행성 관절염 및 류마티스등 보존적 치료술 적용이 불가능 할 경우, 인공무릎관절 전치환술은 무릎관절 기능 회복을 위한 효과적인 치료술로 알려져 있다. 인공무릎관절 전치환술은 환자 초기에 시행하는 1차 인공무릎관절전치환술(Primary total knee arthroplasty)과 1차 전치환술 이후 인공무릎관절의 수명이 다할 때, 재치환 인공무릎관절술(Revision total knee arthroplasty)로 구분되며, 1차 전치환술을 받은 환자의 인공무릎관절 교체 필요성에 따라 재치환 인공무릎관절술

수요도 점차 확대 되고 있다.

세계 인공무릎관절 시장 규모는 약 72억불 시장이며, 이 중 약 10% 내 재치환용 인공무릎관절 시장을 형성하고 있고, 고령화 등으로 인한 인공무릎관절의 수요 증가로 인공무릎관절 시장은 지속적으로 성장하고 있다. 최근 국내에서 1차 인공무릎관절의 개발 및 상용화에 성공하여 임상에 활용되고 있다. 그러나 재치환용 인공무릎관절은 1차 인공관절의 제거와 함께, 골 결손 및 손실이 유발된 무릎관절에 재이식을 해야 하는 어려움과 함께 골 복원, 초기 안정성 확보 및 초기 하중 지지 등 다양한 성능이 요구되어지며, 현재까지 국내에서의 개발은 이루어지지 않고 있다. 이와 더불어 재치환용 인공무릎관절 시장은 소수의 글로벌 인공무릎관절 기업이 해외는 물론 국내 시장을 독점하고 있다.

본 연구에서는 상용화된 일차 인공무릎관절을 바탕으로 재치환용 인공무릎관절 개발에 필요한 임상적, 기계적 성능 요구사항을 분석, 이를 반영한 제품을 설계하고, 다양한 평가를 통해 전량 수입에 의존하고 있는 재치환용 인공무릎관절의 개발을 목표로 하였다. 개발한 재치환용인공무릎관절의 성능 검증을 위해 유한요소 해석 및 기계적 시험 등 생체역학적 안정성 평가와 함께, 생물학적 안전성 평가를 실시하였고, 임상 적용 가능성에 대한 기반을 확보하고자 하였다.

재치환용 인공무릎관절의 성능 요구사항 분석에 따라 설계를 진행하였다. 설계 요소로 1. 안정성(stability), 2. 호환성(modularity), 3. 안전성(safety) 등을 설정하였고, 설계 요소별 세부적인 설계변수를 마련하여 설계를 진행 하였다. 안정성 강화를 위해 인공 무릎관절의 운동 범위를 제한하고, 대퇴부위 관절과 스페이스 관절 굴곡률 값을 높여(conformity) 설계하였다. 호환성 강화를 위해 해부학적 형태를 따라 대퇴부위 및 경골 부위의 주대(extension stem)를 설계하였고, 골 절제량 및 골 손실을 복원하기 위해 부위별 복원 파트를 설계하였다. 그리고 안전성(safety) 확보를 위해 스페이스(spacer)의 후방 모형을 디자인하여, 점프 디스턴스(jump distance)를 증가 시켜 재치환용 인공무릎관절의 탈구를 방지하고자 하였다. 또한 경골 insert locking 및 모듈별 결합

나사 형태를 채기형태로 디자인하였다.

새로 설계한 재치환용 인공무릎관절에 대해 다양한 평가 기법을 활용하여 개발한 제품의 성능 요구사항에 대한 검증을 실시하였다. 인공무릎관절의 구조적 안정성 검증을 위하여 유한요소기법을 활용하여 실시하였다. 경골부 기저판(tibial baseplate) 요소를 제외한 대퇴부 요소 및 insert는 구조적으로 안전한 것을 확인하였고, 기저판은 구조적으로 약 23% 강도가 약화 된 것을 확인하였다. 하지만, 재치환용 인공관절의 설계 요소 인 복원 파트 체결용 hole 설계가 영향을 끼친 것으로 판단되나, 코발트크롬(Co-Cr)의 재질 항복응력 및 인가된 하중을 고려한다면, 인체 삽입 시, 충분히 구조적으로 안정성을 확보할 수 있을 것으로 판단된다. 또한 주대(extension stem)와의 결합 부위에서도 삽입되는 각도에 의해 높은 응력이 발생했으나, 하중 조건등을 고려할 때 결합부위의 안전성에 문제가 없을 것으로 판단된다.

반복된 피로 하중을 받는 인공관절의 특성 상, 피로 하중 특성 및 부품 요소들의 결합력은 시스템의 수명 및 안정성에 중요한 요소들이다. 따라서 안정성 추가 검증을 위해 피로 하중 시험 및 경골부 요소 간 결합력 시험을 실시하였다. 피로 하중 ASTM 시험방법에 따라 피로 하중을 인가하고, 파단의 유무를 평가하고자 하였다. 실험결과, 레벨 8단계에서 천만번의 피로하중 하에서도 파단이나 균열이 발견되지 않았고 이는 체내 이식 후, 반복되는 피로하중 하에서 기계적 안정성에 문제가 없을 것으로 판단된다. 오프셋(offset) 부위와 주대(extension stem)간 결합력 및 풀림력 시험 결과에서도 결합력 대비 풀림력 값이 99%~101%사이를 나타내어 안정성 설계 요소가 반영되었다고 판단된다.

인공무릎관절 시술 이후 인체 내 하중 전달은 생체역학적 안정성 평가에 중요 요소이다. 삽입 시 인공무릎관절로 인한 응력 집중(stress concentration) 및 응력 차폐 현상(stress shielding)은 경골의 추가적 골절이나 통증, 골 흡수로 인한 해리 등을 유발하는 원인으로 알려져 있다. 따라서 재치환용 인공무릎관절이 시술된 유한요소 모델을 개발하여 하중전달 특성에 대해 생체역학적 평가를 하고자 하였다. 우선, 인공

무릎관절이 이식된 유한요소모델을 활용하여 구조적인 안정성 평가를 실시하였다. 이를 위해 재치환용 인공무릎관절 경골부 및 경골(피질골, 해면골)의 응력 분포를 분석하였다. 또한 경골 깊숙이 삽입되는 재치환용 인공무릎관절 경골부가 경골 내에 하중 전달에 미치는 영향을 확인하기 위하여, 경골의 근위부에서 원위 말단부로의 응력/변형률 (stress/strain distribution)을 분석하였고, 추가적으로 상용화된 글로벌 기업의 재치환용 인공무릎관절 모델을 구현하여 하중전달 특성을 비교 분석하였다. 분석 결과, 재치환용 인공무릎관절의 경골부 부위, 피질골 및 해면골에서 실제 항복강도 보다 낮은 응력(PVMS)값을 나타내어 구조적 안정성에 문제가 없음을 나타내었다. 또한 경골 피질골 및 해면골의 응력/변형률 분포를 분석한 결과, 피질골의 응력/변형률 값은 근위부 후방부와 원위 전방부에서 상대적으로 높게 나타났다. 해면골의 경우 근위 후방부 및 원위 외측부에서 높은 응력/변형률 값이 나타났다. 또한 기존 상용화 제품과의 경골 내 하중 및 변형률은 비슷한 패턴을 나타냈으나, 경골 근위부에서는 상대적으로 더 높은 응력 및 변형률 값을 나타내었고, 원위부에서는 상대적으로 적은 하중 및 변형률이 나타났다. 이는 상대적으로 인공관절의 응력 차폐 현상이 기존 제품에 비해 낮은 것으로 판단되고, 골재형성 이내 변형률 값을 나타내어 골 손상 및 안정성에 영향이 없을 것으로 판단된다.

인공무릎관절은 인체 장기간 삽입되는 의료기기로, 새로운 소재가 활용될 경우 생물학적 안전성에 대한 검증이 반드시 확보해야 한다. 기존 티타늄으로 제작하여 활용되던 hole plug를 SL7870이라는 소재를 활용하여 제작하고, 이에 대한 생물학적 안전성(biological safety) 검증을 하였다. 세포독성시험, 피내반응시험, 감작성 시험, 급성독성시험, 유전독성시험을 실시하였다. 세포독성시험 결과 시험군 용출물은 99% 세포 생존률이 관찰되어 세포독성이 없음을 확인하였다. 또한 토끼를 이용한 피내반응 시험 결과, 시험군 용출물은 홍반 또는 부종같은 피부반응을 확인할 수 없었고, 감작성 시험을 통해 쥐의 피부 자극시험에서도 특별한 이상이 없었다. 그리고 급성 독성시험을 통해 피부/기증/눈의 이상과 특이한 행동 양식이 나타나지 않았고, 무게 변화도 감지되지

않았다. 마지막으로 유전독성시험에서도 미생물 돌연변이 유도 결과값이 음성시험군과 차이가 나지 않아, 새로운 소재를 활용한 plug 개발 및 활용에 있어서, 생물학적 안전성에 문제가 없음을 확인하였다.

재치환용 인공무릎관절 개발을 위하여 무릎 관절의 구조적 형태 및 기능에 대해 기초 문헌 조사 연구를 실시하였다. 그리고 인공무릎관절의 특성 및 연구현황에 대해 다양한 문헌 조사를 실시하였고, 본 연구 목표인 재치환용인공무릎관절의 개발을 위해 임상적, 기능적 성능 요구 사항을 분석하였다. 이를 바탕으로 재치환용 인공무릎관절을 설계 하였고, 유한요소 해석, 기계적 시험 등 생체역학적 안정성 평가와 생물학적 안전성 평가를 통해 새로운 재치환용 인공무릎관절의 인체 적용 가능성 및 제품 개발 성공 가능성을 확인 할 수 있었다. 또한 이번 연구를 통해 재치환용 인공무릎관절에 대한 안정성 평가 방법론에 대해 정리 할 수 있었다.

앞으로 인공관절의 특성 상 의료현장에 적용되고 상용화되기까지 다양한 검증 및 지속적인 연구가 이루어져야 한다. 비록 본 연구에서 재치환용 인공무릎관절의 개발을 위해 모든 안전성·유효성 연구를 다 수행하지는 못하였지만, 향후 동역학적 평가, 마모 평가, 장기이식 시험 평가 및 임상시험 연구 등은 반드시 허가 및 상용화에 필수적인 연구들이다. 향후 품목허가를 위해 본 연구 결과를 기반으로 후속 연구를 수행 할 예정이며, 현재 외국 제품이 점유하고 있는 국내 시장 환경 속에서 본 연구 결과는 재치환용 인공무릎관절 국산화 연구에 기반을 제공한 것에 의의가 있을 것으로 사료된다.

키워드 : 인공무릎관절재치환술, 인공무릎관절, 재치환용인공무릎관절, 개발, 설계, 생체역학적 안정성, 생물학적 안전성, 평가, 유한요소기법, 기계시험, 응력